2011

Stem Cell Biology and Strategies for Therapeutic Development in Degenerative Diseases and Cancer

Angel A. Alvarez
University of Central Florida

STEM CELL BIOLOGY AND STRATEGIES FOR THERAPEUTIC DEVELOPMENT IN DEGENERATIVE DISEASES AND CANCER

by

ANGEL A. ALVAREZ
B.S. University of Illinois at Chicago, 2004

A dissertation submitted in partial fulfilment of the requirements
for the degree of Doctor of Philosophy
in the Department of Biomedical Sciences
in the College of Medicine
in the College of Graduate Studies
at the University of Central Florida
Orlando, Florida

Spring Term
2011

Major Professor: Kiminobu Sugaya

ABSTRACT

Stem cell biology is an exciting field that will lead to significant advancements in science and medicine. We hypothesize that inducing the expression of stem cell genes, using the embryonic stem cell gene nanog, will reprogram cells and dedifferentiate human mesenchymal stem cells into pluripotent stem cells capable of neural differentiation. The aims of initial studies are as follows:

Aim 1: Demonstrate that forced expression of the embryonic stem cell gene nanog induces changes in human mesenchymal stem cells to an embryonic stem cell-like phenotype.

Aim 2: Demonstrate that induced expression of nanog up-regulates the expression of multiple embryonic stem cell markers and expands the differentiation potential of the stem cells.

Aim 3: Demonstrate that these nanog-expressing stem cells have the ability to differentiate along neural lineages *in vitro* and *in vivo*, while mock-transfected cells have an extremely limited capacity for transdifferentiation.

Alternatively, we hypothesize that embryonic stem cell genes can become activated in malignant gliomas and differentially regulate the subpopulation of cancer stem cells. This study examines the role of embryonic stem cell genes in transformed cells, particularly cancer stem cells. These studies explore has the following objectives:

Aim 1: Isolate different sub-populations of cells from tumors and characterize cells with stem cell-like properties.

Aim 2: Characterize the expression of embryonic stem cell markers in the sub-population of cancer stem cells.

Aim 3: Examine the effects of histone deacetylase inhibitors at inhibiting the growth and reducing the expression of stem cell markers.

Our research has demonstrated the potential of the embryonic transcription factor, nanog, at inducing dedifferentiation of human bone marrow mesenchymal stem cells and allowing their recommitment to a neural lineage. Specifically, we used viral and non-viral vectors to induce expression of NANOG, which produced an embryonic stem cell-like morphology in transduced cells. We characterized these cells using real-time PCR and immunohistochemical staining and find an up-regulation of genes responsible for pluripotency and self-renewal. Embryonic stem cell markers including Sox2, Oct4 and TERT were up-regulated following delivery of nanog. The role of nanog in the expression of these markers was further demonstrated in our induced-differentiation method where we transfected embryonic stem cell-like cells, that have been transduced with nanog flanked by two loxP sites, with a vector containing Cre-recominase. We tested the ability of these nanog-transfected cells to undergo neural differentiation in vitro using a neural co-culture system or in vivo following intracranial transplantation.

Our next study characterized patient-derived glioblastoma cancer stem cells. We found that cells isolated from serum-free stem cell cultures were enriched for stem cell markers and were more proliferative than the bulk population of cells grown in convention serum-supplemented media. These cancer stem cells expressed embryonic stem cell markers NANOG and OCT4

whereas non-tumor-derived neural stem cells do not. Moreover, the expression of stem cell markers was correlated with enhanced proliferation and could serve as a measure of drug effectiveness. We tested two different histone deacetylase inhibitors, trichostatin A and valproic acid, and found that both inhibited proliferation and significantly reduced expression of stem cell markers in our cancer stem cell lines. These data demonstrate the potential use of stem cell genes as therapeutic markers and supports the hypothesis that cancer stem cells are a major contributor to brain tumor malignancy.

TABLE OF CONTENTS

LIST OF FIGURES

LIST OF TABLES

LIST OF ABBREVIATIONS

AD	Alzheimer’s Disease
ANOVA	Analysis of variance
Bcl	B-cell lymphoma
BrdU	Bromodeoxyuridine
°C	Degrees Celcius
c-MYC	avian myelocytomatosis viral oncogene homolog
Ct	Cycle threshold
Cre	Cyclization recombination
CSC	Cancer stem cell
DAPI	4',6-diamidino-2-phenylindole
DMEM	Delbecco's Modified Eagle's Medium
DNA	Deoxyribonucleic acid
EB	embryoid body
EGF	Epidermal growth factor
eGFP	enhanced Green Flourescence Protein
ESC	Embryonic Stem Cell
FBS	Fetal bovine serum
FGF	Fibroblast growth factor
FITC	Fluorescein isothiocyanate
GAPDH	Glyceraldehyde 3-phosphate dehydrogenase
GBM	Glioblatoma
GFAP	Glial fibrillary acidic protein
h	Human
HDACi	histone deacetylase inhibitors

HPRT	hypoxanthine- guanine phosphoribosyltransferase
Lox P	Locus of X-over P1
m	Mouse
MAP2	Microtubule-associated protein 2
MCM2	mini-chromosome maintenance protein 2
MSC	Mesenchymal Stem Cell
NSC	Neural Stem Cell
Oct4	Octamer-binding transcription factor 4
PBS	Phosphate-buffered saline
PCR	Polymerase chain reaction
PFA	Paraformaldehyde
RNA	Ribonucleic acid
RT-PCR	Real-time polymerase chain reaction
SD	Standard deviation
Sox2	SRY (sex determining region Y)-box 2
SSEA	Stage-Specific Embryonic Antigen
SV40T	Simian virus large T antigen
TERF1	Telomeric repeat-binding factor 1
TERT	Telomerase reverse transcriptase
TRITC	Tetramethyl Rhodamine Isothiocyanate
TSA	Trichostatin A
UTR	Un-translated region
VPA	Valproic Acid
VSV-G	Vesicular stomatitis virus glycoprotein
ZFP342	Zinc finger protein 342

CHAPTER ONE:
NANOG OVEREXPRESSION ALLOWS HUMAN MESENCHYMAL STEM CELLS TO DIFFERENTIATE INTO NEURAL CELLS

Chapter Summary

Stem cell therapies have been proposed as a treatment option for degenerative disease, like Alzheimer's disease (AD), but the best stem cell source and their therapeutic efficacy remain uncertain. Embryonic stem cells (ESCs) can efficiently generate multiple cell types, but pose ethical and clinical challenges, while the more accessible adult stem cells have a limited developmental potential. The primary objective of this article is to show that following over-expression of an ESC gene, nanog, adult human mesenchymal stem cells (HMSCs) could be dedifferentiated into cells exhibiting ESC characteristics based on morphology, immunohistochemical staining, and gene expression. After expansion, nanog-transfected HMSCs had the potential to be directed toward neural cell lineage under influence of conditional media from differentiated human neural stem cells using a membrane-separated co-culture system. Recommitted cells differentiated into cells immunopositive for βIII-tubulin and glial fibrillary acidic protein, indicating the presence of neurons and astrocytes, respectively. We further demonstrated the ability of dedifferentiated HMSCs to survive, migrate, and undergo neural differentiation in vivo in rodents. This data offers an exciting prospect that adult cells can be modified and used to neurodegenerative conditions.

Introduction

Dementia is a serious medical illness that affects an estimated 24.3 million people worldwide[1] at a cost of $315.4 billion annually[2]. Severe cognitive impairment from Alzheimer's disease (AD) is associated with the majority of dementia cases. While most pharmacological treatments for AD fail to improve cognition, several lines of evidence suggest that neuro-replacement therapy may reverse cognitive impairment. Namely, neurogenesis is associated with cognition and is congruously impaired with aging.[3, 4] Second, neural stem/progenitor cell proliferation and differentiation are significantly diminished in AD and Down's syndrome models both in vitro and in vivo.[5-8] Finally, cognitive performance improves through increasing neurogenesis from an enriched environment[9-11], pharmacological treatment[11, 12], or following stem cell transplantation[12-16]. Although Gallagher's group failed to show a relationship between neurogenesis and cognition in a normal aging rodent model,[17, 18] the collective body of evidence suggests that neurogenesis is important for maintenance of normal brain function.

Embryonic stem cells (ESCs) have been proposed as treatment for neurodegenerative diseases because of their pluripotency, but concerns over ethics[19-21], immune response[22-24] and tumor formation[25-28] have been major barriers for their clinical use. Utilization of adult stem cells could eliminate these issues because they can be harvested from a patient and autologously transplanted back to the patient. However, the ability of adult

stem cells, such as human bone marrow-derived mesenchymal stem cells (HMSCs), to develop along multiple lineages is limited. Although studies have claimed that HMSCs transdifferentiate into cells outside their restricted germ layer, the transdifferentiation could have been from a very limited population of HMSCs[29-31] or due to the low frequencies of cell fusion, which allow MSCs to acquire characteristics of multiple cell types by fusing to somatic cells.[32-34] Therefore, a strategy to increase the potency of adult stem cells is requisite for their use in neurotherapy.

In a prior study, we demonstrated that HMSCs treated with bromodeoxyuridine (BrdU) undergo neural differentiation following transplantation in the brains of rats and improve cognitive function.[13] However, efficiency of transdifferentiation and concerns with the use of BrdU, which is incorporated into the DNA as a thymidine analog, led us to explore other strategies.

One possible strategy is cell fusion that would alter the characteristics of the adult stem cells based on the exogenous cell used for merging. This method could change the potency of cells allowing them to develop into cells beyond their respective lineage.[35-38] The fusion of somatic cells to ESCs prompts expression of the embryonic stem cell gene Oct-4.[38, 39] Thus, the expression of stem cell genes that regulate self-renewal and pluripotency may play an integral role in reprogramming the cell lineage.

Earlier studies have indicated that the expressions of critical stem cell genes are capable of maintaining ESCs in a pluripotent state. The suppression of ESC differentiation has been demonstrated with the over-

expression of ESC genes including nanog[40, 41], Pem[42] and Rex1[43], although the presence of elevated levels of Oct-4 was insufficient to guard against ESC differentiation.[44] In this study, we tested our hypothesis that developmental potency of MSCs can be gained by changing the gene expression profile through the over expression of nanog, and the resulting cells can be transdifferentiated into neural cells. This technology may allow us to use patients' own HMSCs to treat neurodegenerative diseases, such as AD.

Materials and Methods

Cell Culture

Adult human bone marrow-derived HMSCs (Cambrex) were cultured in DMEM (Invitrogen) supplemented with 1% antibiotics (Invitrogen) and 10% FBS for improved HMSC growth (StemCell Technologies). Per Cambrex product information, mesenchymal stem cells are harvested and cultured from normal human bone marrow. Cell purity is far higher than cells from traditional Dexter cultures. Cells are tested for purity by flow cytometry and for their ability to differentiate into osteogenic, chondrogenic and adipogenic lineages. Cells are positive for CD105, CD166, CD29, and CD44. Cells test negative for CD14, CD34 and CD45. Media systems are available to support growth of HMSCs, and their differentiation into adipogenic, chondrogenic, and

osteogenic lineages. Cells were cultured in T75 tissue culture treated flasks (BD Biosciences) and incubated in a CO2 chamber at 37℃ with 5% CO2 (NuAire). Co-culture experiments were carried out using differentiated NSCs in Falcon tissue culture treated 6-well plates (BD Biosciences). Prior to co-culture, fetal-derived human NSCs (Cambrex) were expanded in serum-free NSC medium of DMEM/F12 (Invitrogen) supplemented with B27 (1:50, Invitrogen), basic Fibroblast Growth Factor (bFGF, 20 ng/ml, R&D Systems), Epidermal Growth Factor (EGF, 20 ng/ml, R&D Systems), heparin (0.18 U/ml, Sigma), and 1% antibiotics (Invitrogen). Cells were allowed to spontaneously differentiate for one week in tissue culture treated 6-well plates containing serum-free neural basal medium.

For co-culture, cell culture inserts with a semi-permeable membrane with 0.4 μm pores (BD Biosciences) were used to separate the Nanog-transfected HMSCs from the differentiated HNSCs. This allowed for the dynamic exchange of secreted factors and eliminated direct cell contact to avoid possible cell fusion. Nanog- or mock-transfected HMSCs were then transferred to co-culture to promote neural differentiation. To eliminate Nanog expression in viral-loxP-Nanog-transduced HMSCs prior to the co-culture, plasmids containing the Cre recombinase gene regulated by an EF1α promoter (Addgene, plasmid 11918) were transfected into the cells using the FuGene 6 reagent. Cells were allowed to differentiate for 10 days and then stained for early (βIII-tubulin) and mature (MAP2) neuronal markers and astrocytic markers, GFAP and S100.

Cloning of Nanog Gene

Nanog was originally cloned from male genomic DNA that was pre-digested with the restriction enzymes NotI, XbaI, and SpeI, then amplified by PCR using Nanog-specific primers, (CGTTCTGCTG- GACTGAGCTGGTT, CGGGCGGATCACAAGGTCAG). PCR conditions consisted of pre incubation at 94℃ for three minutes, 30 cycles consisting of 94℃ for one minute, 52℃ for 30 seconds, and 72℃ for three minutes, and post dwells at 72℃ for 10 minutes. The PCR pro- duct was then placed into a mammalian expression vector (TopoHisMax 4.1, Invitrogen) according to manufacturer's protocol. The cloned sequence was confirmed by DNA sequencing.

Production of Lentivirus Containing Nanog

The gene encoding for Nanog (gift from Austin Smith, MD University of Cambridge) was amplified using the Herculase II fusion DNA polymerase (Promega) and gene-specific primers containing a BamHI enzyme-cutting site in the forward primer and a SalI-cutting site in the reverse primer (ATAGGGATCCACATGAGTGTTGACCCAGCTT, ATAGGTCGACTCACACGTCTTCAGGTTGCA). The PCR amplified Nanog was sub-cloned into the pLox lentiviral vector (gift from Didier Trono, MD and Patrick Salmon, MD, LVPU, Centre Médical Universitaire, Genève, Switzerland).

Production of a lentiviral vector containing the Nanog sequence was carried out using a vector containing a LoxP site. The pLoxNanog vector, the packaging vector pCMVΔR8.91 (AddGene) encoding for regulatory proteins Tat and Rev as well as the Gag and Pol precursors, and a vector for the envelope protein VSV-G (Clontech) were used for viral production. The aforementioned vectors and lentiviral vectors pLoxNanog and pLoxGFP, combined with the packaging and envelope plasmids at a ratio of 2:1:1 (pLox:pCMVΔR8.91:pVSV-G) [45, 46], were transiently transfected into the HEK293T/17 cell line (ATCC) using Lipofectamine (Invitrogen) at a DNA (20µg) to Lipofectamine ratio of 1:2.5. The cell culture media was removed at 24 hours and collected every 12 hours thereafter for the next two days to harvest the viral supernatant.

Non-viral and Viral Gene Delivery

For non-viral gene transfection, 75% confluent HMSCs were transfected with 3µg of Nanog vector using two different reagents, Neuroporter (Gene therapy systems) or FuGene 6 (Roche), at DNA to reagent ratios of 1:15 and 1:3, respectively. Proliferative clusters began to emerge after one week and grew large enough for expansion typically by three weeks. Clustered cells that resembled Nanog-transfected HMSCs were passed by mechanical dissociation from the feeder layer and subsequently plated with a feeder cell layer of HMSCs.

For lentivirus-mediated transfection, viral supernatant was transferred to HMSC cultures for viral transduction. Delivery of Nanog was analyzed through fluorescent microscopy for positive green fluorescent protein (GFP) expression. Differentiation was induced through the deletion of the Nanog-containing proviral sequence with a vector encoding for Cre recombinase (Addgene pBS513)[47-49]. The Cre vector, which contains an EF1α promoter, was delivered to the cells through chemical transfection. Following Cre-transfection, cells were used for neural differentiation or gene expression analysis at 72 hours post-transfection. All recombinant DNA research was performed in accordance with NIH guidelines.

Gene Expression Analysis

RNA extraction was performed using TRIzol (Invitrogen) according to manufacturer's instructions. Media was removed from cultured cells and incubated with 1ml of TRIzol for five minutes at room temperature. The TRIzol solution was phase-separated by an addition of chloroform, thoroughly mixed, and centrifuged at 11,500g for 15 minutes. The RNA was precipitated from the top aqueous phase by isopropanol, centrifuged at 11,500g for 10 minutes, and the RNA pellet was washed with 75% ethanol. The RNA-ethanol solution was centrifuged for five minutes at 7,400g, the supernatant removed, and the pellet was re-suspended in molecular biology grade water. RNA concentration were measured based on absorption and converted to cDNA for PCR

analysis. Reverse transcription was performed using an iScript cDNA synthesis kit (Bio-Rad).

Primers used for RT-PCR were GAPDH (AGCCACATCGCTCAGACACC, GTACTCAGCGGCCAGCATCG), β-actin (TCCTGAGCGCAAGTACTCC, AAGCATTTGCGGTGGACGA), Nanog (ACAACTGGCCGAAGAATAGC, AGTGTTCCAGGAGTGGTTGC), Oct-4 (CTTGCTGCAGAAGTGGGTGGAGGAA, CTGCAGTGTGGGTTTCGGGCA), TERF1 (GCAACAGCGCAGAGGCTATTATT, AGGGCTGATTCCAAGGGTGTAA), Sox-2 (ATGCACCGCTACGACGTGA, CTTTTGCACCCCTCCCATTT), ZFP342 (GAAGGCATCACCCAAAAAGA, GCGGTTGAGCTTACTGCTCT), TERT (CGGAAGAGTGTCTGGAGCAA, GGATGAAGCGGAGTCTGGA), and eGFP (CCTGAAGTTCATCTGCACCA, GGTCTTGTAGTTGCCGTCGT).

Real-time two-step RT-PCR was performed using a SYBR green PCR mix (Bio Rad), carried out in a My-IQ iCycler (Bio Rad) and then analyzed by the ΔCt method as previously described [50, 51].

Stem Cell Transplantation

Two different transplantation studies were performed with C57/Black mice at four months of age in accordance with approved protocols from the University of Central Florida's Institutional Animal Care and Use Committee.

The animals were fixed in a stereotaxic apparatus and approximately 1x10^5 cells in 10µl of phosphate-buffered saline (PBS) were slowly injected into the right lateral ventricle (coordinates: AP -1.4, ML 1.8, DV 3.8). Experiments were carried out independently using HMSCs dedifferentiated through non-viral transfection or lentiviral transduction.

Stem Cell Transplantation

Two different transplantation studies were performed with either six eight-month Fisher 344 rats for non-viral dedifferentiated cells or C57/Black mice for virally-transduced cells for transplantation in accordance with approved protocols from the University of Central Florida's Institutional Animal Care and Use Committee. Prior to transplantation, animals were anesthetized with intraperitoneal injections of a solution mixture of ketamine hydrochloride and xylazine (X-Ject) (1:1 ratio). Adequate sedation was determined by a lack of palpebral and tail-pinch reflexes.

Once properly sedated, animals were set atop a platform of appropriate height and secured within a stereotaxic apparatus using the nose clamp and ear bars. The heads of the animals were shaved and an anterior to posterior incision was made with a surgical scalpel to reveal the skull. Using bregma as a reference, the location of the right lateral ventricle was located using a brain atlas, and a needle hole was carefully drilled through the skull but not into the brain. Approximately 1x10^5 cells in 10µl of phosphate-buffered saline (PBS)

were slowly injected into the right lateral ventricle (coordinates: AP -1.4, ML 1.8, DV 3.8). Cells in solution were kept on ice and adequately re-suspended to avoid cell aggregation. Experiments were carried out independently using HMSCs dedifferentiated through non-viral transfection or lentiviral transduction. Following injection, residual blood was gently cleaned with sterile cotton swabs and the incision closed using surgical clamps. Animals were post-surgically monitored for signs of bleeding, infection, and behavioral changes.

Brain Sample Preparation

Animals were deeply anesthetized and perfused using a 10% sucrose solution followed by fixation with a 4% paraformaldehyde PBS (pH 7.2). Following fixation, brains were removed and placed inside a 20% sucrose/4% paraformaldehyde solution and left overnight at 4℃. When the brain settled to the bottom of the container, it was froze in isopentane pre-cooled by submerging the beaker into liquid nitrogen. The brains were mounted using a cryomedium, sliced into 20μm sections using a cryostat at –20℃ and collected in PBS and stored at 4℃ until antibody staining.

Immunocytochemistry and Immunohistochemistry

Cultured cells were washed with PBS then fixed with a 4% buffered paraformaldehyde (Sigma) solution overnight at 4℃. Following fixation, cells were washed with PBS (Sigma) then permeabilized with PBS-Tween (Sigma) containing 0.1% Triton-X (Fisher Scientific) for one hour at room temperature. Brain sections were washed with PBS then permeabilized by incubation in PBS-Tween with 0.1% Triton-X at room temperature for one hour. The samples were then incubated for one hour at room temperature in a blocking solution of PBS-Tween with 3% donkey se-rum (Jackson ImmunoResearch). Primary antibodies TRA-1-60 (MAB4360), SSEA-3 (mab4303), Sox-2 (AB5603), MAP2 (AB5622), and Oct-4 (mab4305) all from Chemicon, Nanog (AF1997, R&D Systems), βIII-tubulin (T8660, Sigma), S100 (S2644, Sigma), and GFAP (G9269, Sigma) were added to blocking solution and incubated overnight at 4℃. The next day, samples were washed with PBS and incubated in the dark with FITC- or TRITC-conjugated secondary antibodies at room temperature. Samples were washed with PBS, cover-slipped with water-based mounting solution containing DAPI (Vector Laboratories), and sealed using clear nail polish.

Results

Cloning of nanog: Sequence analysis showed over 99% sequence identity with nanog but did not contain introns, suggesting that it may be nanog pseudogene 8 (NANOGP8),[52] one of twelve nanog variants.[52-56] The high homology and intact coding region suggests that the cloned sequence should be indistinguishable from nanog and the translated product virtually identical to the actual nanog protein, with the exception of substitutions occurring in residues 16 and 253, changing alanine and glutamine for glutamate and histidine, respectively. The cloned gene sequence can be segmented into seven distinct regions: the 5' untranslated region (UTR), N-terminal domain, homeodomain, C1 domain, Cw domain, C2 domain, and the 3' UTR. The 5' region contains binding sites for embryonic stem cell genes Oct-4 and Sox-2, which are part of a transcriptional regulatory loop.[57-60] The 5' region also contains a p53-binding site within the nanog promoter region that facilitates ESC differentiation[61] and is possibly responsible for the shift in replication timing observed with neural differentiation.[62] The N-terminal region of nanog has transcriptional activity[63] and encodes for a sequence containing a SMAD-binding domain.[54, 64] The homeodomain portion is similar to the NK-2 and ANTP family of homeodomain transcription factors, but comparing 120 different homeodomain proteins using BLOcks SUbstitution Matrix (BLOSUM) and Point Accepted Mutation (PAM) matrices suggests that nanog represents a distinct protein family divergent from both the NK-2 and distal-less gene family

(data not shown). The C-terminal domain contains no apparent transactivation motifs, but has greater transactivation activity compared to the N-terminal and homeodomain.[63, 65]

The C-terminal domain can be subdivided into three regions: the portion immediately following the homeodomain region (C1), the subregion containing a unique repeated motif of tryptophan flanked with four polar-uncharged amino acids (Cw), and a more distal sequence (C2). Cloning of nanog inside the pLox lentiviral vector was successful and DNA sequencing confirmed a match for the actual nanog gene. The nanog sequence was properly inserted into the vector containing LoxP sequence within the long tandem repeat, allowing for efficient proviral deletion following delivery of Cre recombinase.[55, 56]

Transfection of nanog: In the current study, human bone marrow HMSCs were cultured and grown to 75% confluence and treated with a plasmid containing nanog or served as mock-transfected control. Following optimization, we achieved transfection rates of less than 5% using non-viral transfection. Nanog transfection altered the morphology of cells, producing smaller proliferative cells that themselves formed clusters (Figure 1, A).

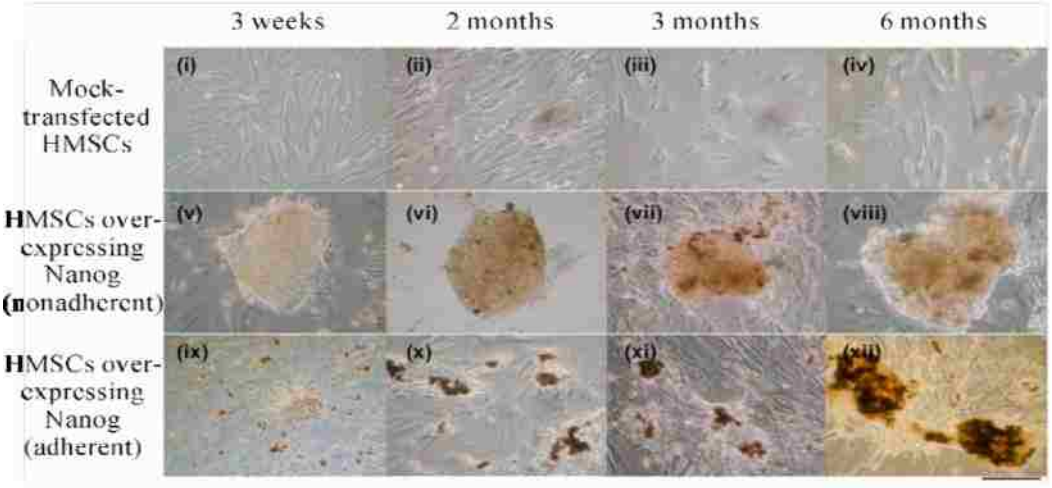

(a)

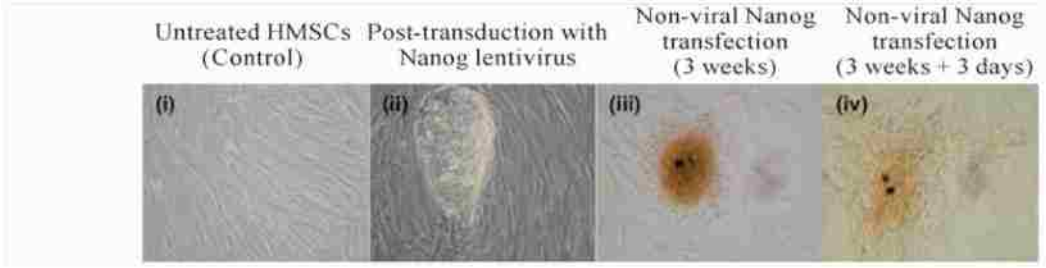

(b)

Figure 1: (a) HMSCs over-expressing Nanog displayed ESC-like (v-viii) or EB-like morphology (ix-xii). Morphological changes seen at three weeks (i,v,ix), two (ii,vi,x), three (iii,vii,xi), and six months (iv,viii,xii) post-transfection. (b) HMSCs nine days post-transduction with Nanog lenti-virus (ii). Three weeks following non-viral Nanog transfection (iii) and three days later (iv). Untreated HMSCs showed as a control (i).

Two basic cell types were observed; namely, the proliferative clusters tended to form either an adherent mass of cells that were ESC-like or more spherical, non-adherent/loosely adherent clumps somewhat resembling embryoid bodies (EB-like). The EB-like cells originated as small, scattered clumps, but formed larger aggregates within weeks. These larger clusters were mainly the result of clump aggregation rather than cell proliferation.

Transfection with the neuroporter reagent appeared to have more toxicity and was more likely to produce EB-like cells, therefore FuGene 6 was the preferred transfection reagent. Cells that displayed the flattened, ESC-like morphology were detected as early as one week, but were usually distinct at two to three weeks. The number of colonies produced did not appear to directly correspond to transfection rates. Following one week, one or two colonies could be observed in the wells. No colonies were able to expand without a feeder layer, and only a few colonies were able to expand into larger colonies of thousands of cells for subsequent passaging.

Moreover, the colonies that did form and display ESC-like morphology were only found within the nanog-transfected cell cultures. Both of the previously defined cell types either adhered and differentiated or underwent cell death when transferred to separate culturing flasks with no feeder layer (data not shown). The inability of isolated colonies to continually proliferate on their own indicates that the majority of non-transfected HMSCs served as a feeder layer, helping provide growth factors and aid in cell survival. ESC-like colonies were less homologous and displayed greater propensity for differentiation than has been reported with ESCs (Figure 1A).

There was little difference between ESC-like cells and ESCs for up to two months in culture, and while they were able to proliferate, they did not appear to grow past 1000μm. However, by three months, gradual changes became evident as heterogeneity within the structures became more apparent. It is uncertain whether this phenomenon is the result of cells undergoing differentiation, reaching a proliferative limit, or the result of changes in the underlying feeder layer of un-transfected HMSCs. Control HMSCs showed changes in morphology at three months in culture, and by three months displayed little or no proliferation.

Beyond three months, the number of nanog-transfected ESC-like cells diminished, and mock-transfected HMSCs showed age-related alterations. HMSCs could be cultured for longer periods of time through continuous passages, but late-passaged HMSCs displayed changes in morphology, including increased cell size, larger cytoplasm, and no detectable proliferation. Following one year of culturing and expansion, HMSCs failed to survive and few ESC-like cells remained.

Cells co-transduced with nanog and GFP lentiviruses showed prominent cluster formation (Figure 1B). Colonies formed by transduction with nanog were easier to maintain and grew much larger than HMSCs chemically transfected with nanog. Colonies produced through chemical transfection were difficult to maintain as the colonies tended to disperse (Figure 1B).

Gene expression and immnohistochemistry of nanog-transfected HMSCs: Exploring biochemical changes following nanog transfection, we performed RT-PCR for nanog and Oct-4 to compare with mock-transfected

HMSCs, as well as immunostaining for known embryonic stem cell markers. Expression levels of nanog and Oct-4 were absent or low in two different batches of mock-transfected HMSCs (Figure 2).

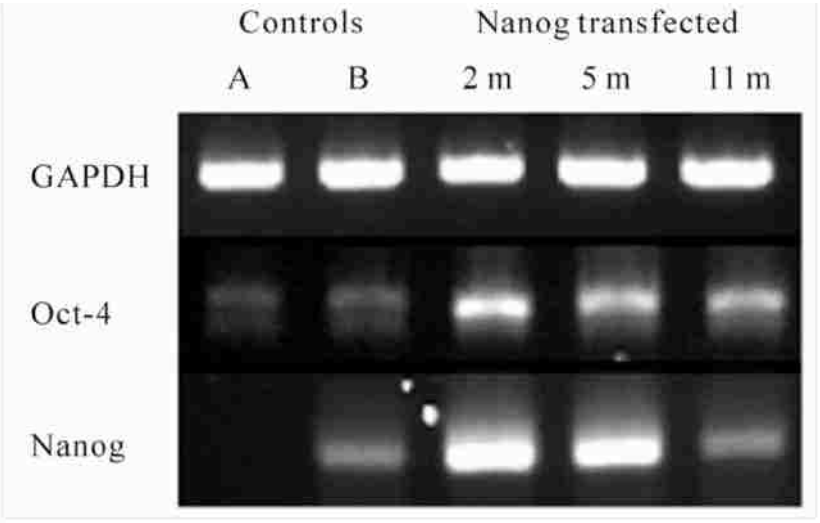

(a)

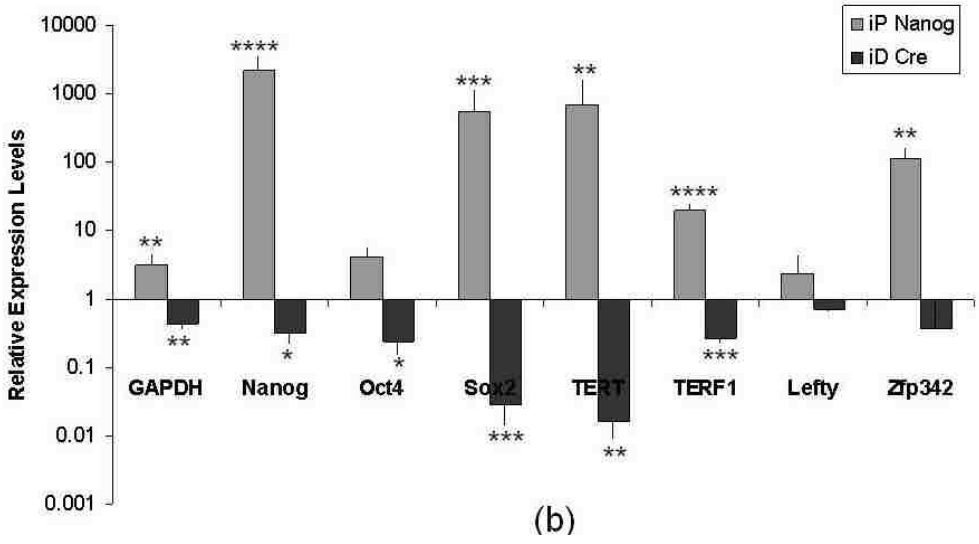

(b)

Figure 2: (a) RT-PCR shows little or no expression of Nanog and Oct-4 in mock-transfected HMSCs but up-regulation of both at two, five, and eleven months following Nanog transfection up to 11 month in a culture. GAPDH was a control. (b) qRT-PCR of Nanog lentiviral-transduced cells. Up-regulation of multiple ESC genes after Nanog transfection (grey) were observed and these genes were down-regulated after (black) delivery of Cre recombinase vectors to remove Nanog expression.

This illustrates the heterogeneity of HMSCs in culture and is consistent with the data showing a subpopulation of pluripotent HMSCs.[29-31, 66, 67] Following nanog transfection, expression of both nanog and Oct-4 were highly elevated at two, five, and eleven months. It was unexpected that either nanog or Oct-4 would be expressed following long-term expansion since the few remaining cell clusters did not appear to proliferate at one year. Interestingly, levels of Oct-4 did not directly correlate with expression of nanog, which is consistent with findings that Oct-4 is not directly controlled by nanog.[57, 58, 68]

Quantitative gene expression analysis was difficult given the heterogeneous population and relatively low frequency of nanog-transfected cells. We therefore attempted to select out nanog-dedifferentiated cells using a lentiviral system and green fluorescent protein. Using lentiviruses to deliver nanog and GFP, we created dedifferentiated cells that were more homogenous, highly proliferative, and easily expandable. In fact, the cells were able to grow with or without feeder cells for over 40 passages.

Quantitative real-time PCR was performed on lentiviral-transduced cells and showed a dramatic increase in most of the ESC genes tested. We were able to detect low levels of both nanog and Oct-4 in two of three HMSC batches tested, but telomerase expression was absent. Following forced expression of nanog, we measured dramatic increases in nanog, Sox-2, zinc-finger protein 342, TERF1 and telomerase. Given the lack of telomerase expression, we assigned the lowest value for detection in order to perform an analysis that does not allow for “zero” expression. We observed only a

modest, yet statistically significant, increase in levels of Oct-4 to four times the normal level (Figure 2). The measured changes, particularly the sudden expression of telomerase and increase in TERF1, demonstrate fundamental changes in the HMSCs following delivery of nanog. Previous work has revealed that human HMSCs fail to express telomerase and have a unique telomerase biology compared to other stem cells,[69, 70] so the link between nanog and telomerase is an exciting area that warrants exploration.

Removing nanog and GFP using a vector encoding for the Cre recombinase enzyme should reverse gene expression changes in the viral-transduced cells. Recombination and gene excision was successful, as most viral-transduced cells were negative for GFP post-Cre transfection, allowing for neural differentiation. Additionally, real-time PCR reveals an 89% decrease in GFP expression in viral-transduced cells 72 hours following delivery of Cre (data not shown). We compared changes in gene expression changes in Cre-transfected, virally-dedifferentiated cells and found reduction in most stem cells genes. Nanog, Oct4 and TERF1 showed a 70% to 80% decrease in expression, while Sox-2 and telomerase showed decreases of approximately 98% each (Figure 2b).

Immunohistochemical staining was performed using antibodies against the ESC markers nanog, Oct-4, stage-specific embryonic antigen-3 (SSEA3), and keratan sulphate-associated antigen TRA1-60. If nanog dedifferentiates HMSCs, transfected cells should stain positive for ESC markers. The vast majority of untreated cells failed to stain for any ESC markers, but a small population (approximately 1%) of cells, did show positive staining for

transcription factors Oct-4 and nanog, while faint staining for surface markers was seen in about 5% of cells (Figure 3). Alternatively, nanog-transfected cells did display positive staining for the ESC transcription factors nanog and Oct-4 within the proliferative cell clusters, although not in the surrounding feeder layer of HMSCs. Nanog-transfected cell clusters also showed positive expression of ESC surface markers SSEA3 and TRA1-60 (Figure 3).

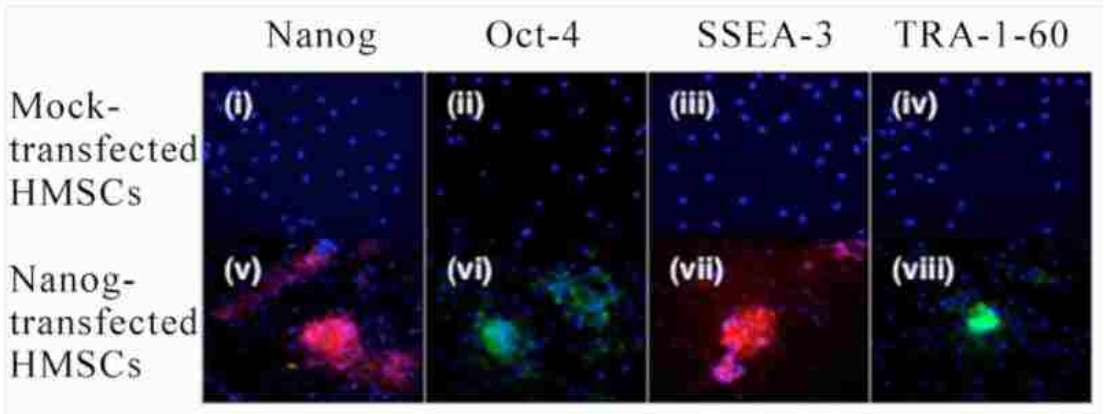

Figure 3: Immunocytochemistry of Nanog transfected HMSC colonies showed strong immunoreaction for ES cell markers after15 weeks in a culture (v-viii) while there is no expres- sion of ES cell markers in mock-transfected HMSCs (i-iv). The cells were immunostained for Nanog (i, v), Oct-4 (ii, vi), SSEA-3 (iii, vii), and TRA-1-60 (iv, vii).

This staining pattern was more apparent with the use of the GFP and nanog lentiviral-transduced cells. Following transduction with nanog and GFP, large ESC-like colonies began to form. GFP expression appeared localized to ESC-like colonies and showed positive staining for manog and Sox-2, unlike non-treated HMSCs (Figure 3B). Taken together, it appears that forced expression of nanog results in the dedifferentiation of HMSCs and induces the expression of ESC markers.

We next tested the ability of nanog-transfected cells to undergo neural differentiation using a previously established co-culture system. Dedifferentiated cells were placed in co-culture consisting of a feeder cell layer separated by a semi-permeable membrane to eliminate direct cell contact. The feeder cells used were neurons and glial cells derived from human neural stem cells, and were grown as neural spheres and cultured in serum-free basal media. This system allows for the exchange of growth factors and eliminates the concern over cell fusion since it prevented direct cell contact between the HMSCs and underlying feeder cells. Cell clusters adhered to the membrane surface and differentiation occurred as cells radiated outwards. Control HMSCs adhered to the membrane surface but failed to differentiate into neurons and astrocytes. The differentiation pattern was tested by immunostaining against βIII-tubulin and GFAP, neuronal and astrocytic markers, respectively (Figure 4).

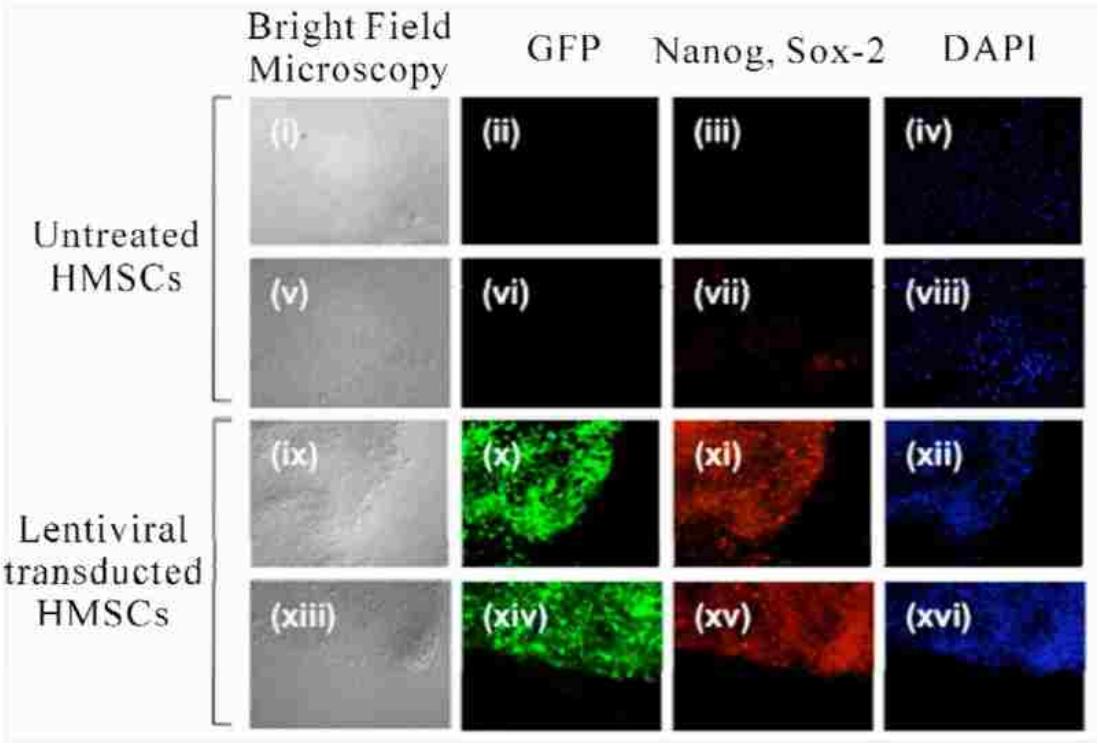

Figure 4: With mock-transfected HMSCs showed no ESC- like colony formation (i,v) nor GFP expressions (ii,vi) and immunoreactivities for Nanog (iii) and Sox-2 (vii) are not detected. Lentiviral transduction with Nanog and GFP in- duced colony formation (ix, xiii) and GFP expression (x, xiv), and positive for Nanog (xi) and Sox-2 (xv) immunore- activities. DAPI is used counter stain of nuclei (iv, viii, xii, xvi).

The un-transfected HMSCs did not show positive staining for the neuronal marker βIII-tubulin, but approximately two percent of the cells did show weak expression of GFAP. This may represent a subpopulation of pluripotent HMSCs[30, 66] that is capable of differentiating into astrocytes. Modified cells formed spherical clusters with a similar appearance to differentiated neural stem cells, forming a web-like network of neurons and astrocytes that stained positive for both βIII-tubulin and GFAP (Figure 5). However, βIII-tubulin and GFAP are early lineage commitment markers, so we examined the expression of MAP2 and S100 to determine if these mature neuronal and astrocytic markers would be expressed following neural differentiation to our dedifferentiated cells. Induction of differentiation in the viral-transduced cells was achieved by first transfecting the cells with a vector encoding for Cre recombinase, then placing the cells in conditioned media for neural differentiation. Cre-transfection was successful, as evident by the majority of cells now being GFP negative. We found that some cells did show positive staining for both markers, and most cells were negative for GFP (Figure 6).

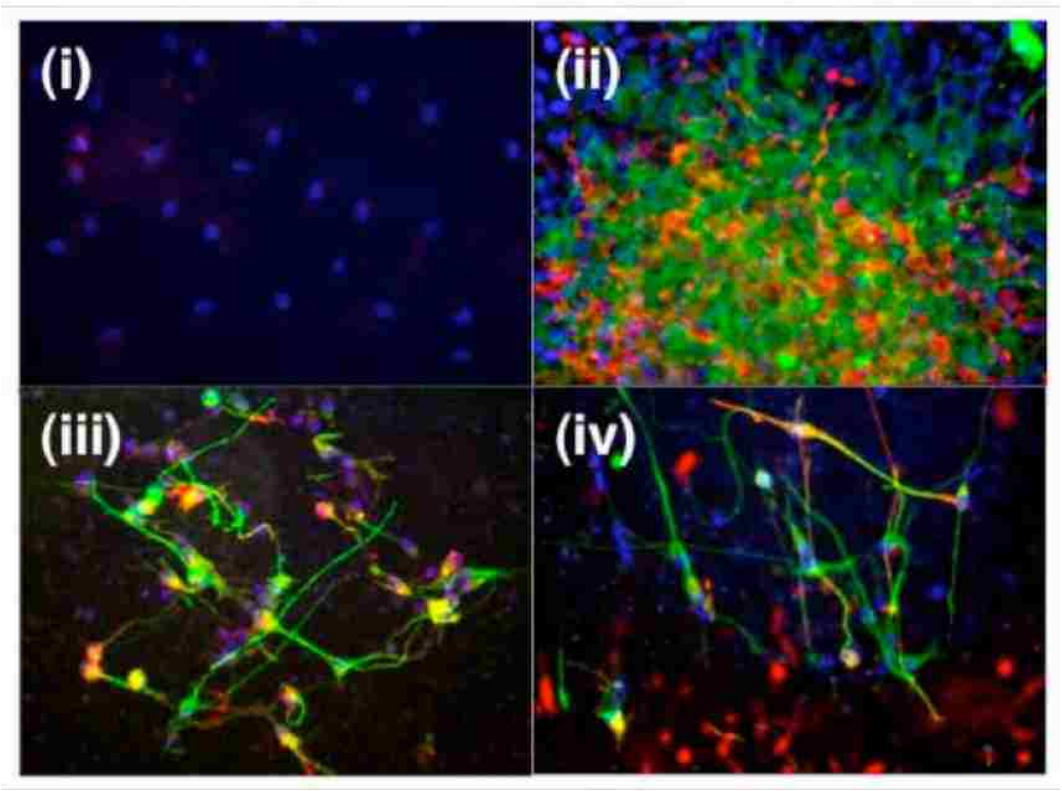

Figure 5: After co-culture with differentiated human neural stem cells, naive HMSCs showed few GFAP (red) but no βIII-tubulin (green) immunoreactivites (i). While Nanog- transfected HMSCs forming clusters of cells co-cultured with differentiated human neural stem cells attached to the culture insert membrane and migrated outward. They were positive for GFAP (red) and βIII-tubulin (green) immunoreactivites indicating neural differentiation of the cells, (low magnification in ii, high magnification in iii). Differentiated Nanog-transfected HMSCs are also stained positive for MAP2 (green) and S100 (red) at two weeks, indicating differentiation into mature neurons and astrocytes, respectively.

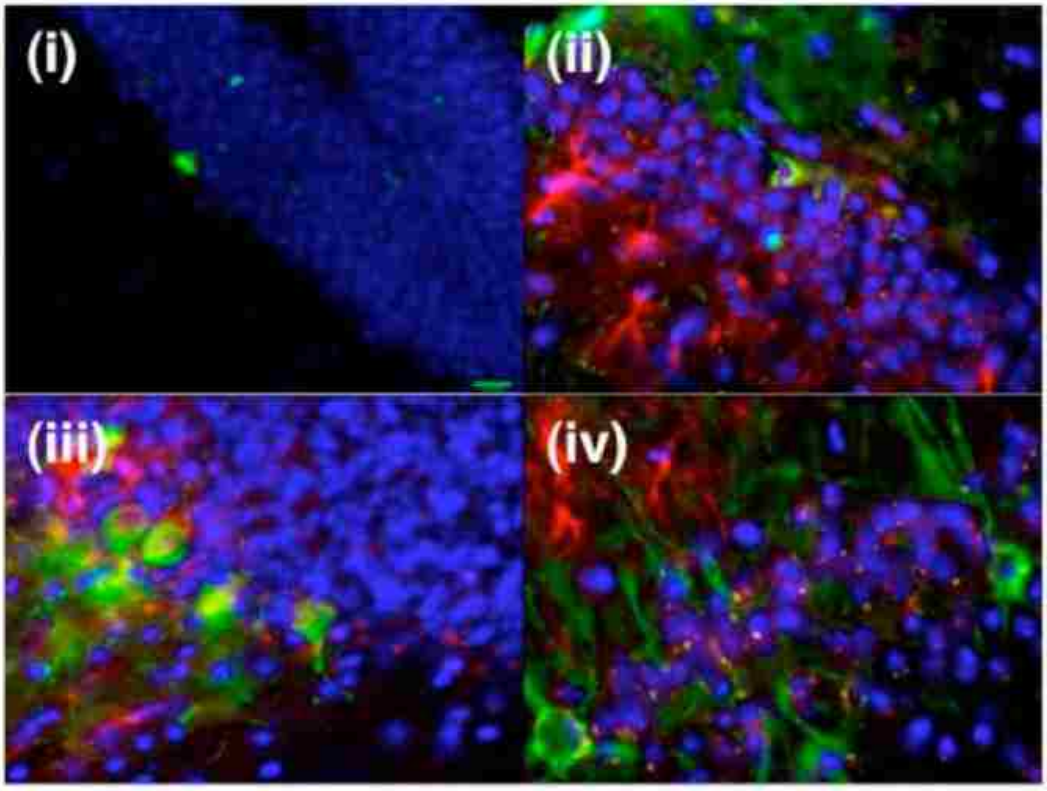

Figure 6: After transplantation into mice, Nanog-GFP transfected HMSCs HMSCs are capable of migration into hippocampus dentate gyrus (i). Immunostaining specific to human βIII-tubulin (green) and GFAP (red) indicated that the transplanted Nanog-transfected HMSCs after Cre recombinase treatment differentiated into neurons and astrocytes in the dentate gyrus (ii, iii) and CA1 regions (iv) of the hippocampus, respectively.

Immunohistochemical staining shows expression of early neuronal (βIII-tubulin) and astrocytic (GFAP) markers at three days in neural differentiation culture. Cells were cultured for two weeks and stained for mature neural markers. Cells stained positive for MAP2 and S100, indicating the cells were able to express mature neuronal and astrocytic makers, respectively.

Transplantation results: We tested the cell fate and migration of non-viral and lentiviral dedifferentiated HMSCs in vivo three weeks post-transplantation. Following sacrifice, the brains were sectioned and examined. None of the animals displayed evidence of tumors, but a separate cluster of cells was observed in one region of brain sectioning, presumed to be from the original transplantation. Immunohistochemical staining for human βIII-tubulin and GFAP did reveal evidence of both in vivo neuronal and glial differentiation. Moreover, the presence of transplanted cells, marked by the expression of human neural markers or GFP in the Cornu Ammonis fields of the hippocampus proper and dentate gyrus regions, is encouraging given the role of these structures in learning and memory (Figure 6).

The high frequency of transdifferentiation demonstrates a new technology that neither relies on cell fusion nor the enrichment of low frequency subpopulations of cells that can be applied for neuroreplacement therapies.

Discussion

This study demonstrates a novel method of dedifferentiating adult stem cells by over-expressing genes regulating pluripotency, with the end goal of facilitating neural transdifferentiation of HMSCs, which may allow us to perform autologous cell therapies for individuals with AD and other neurodegenerative diseases. Nanog transfection of HMSCs produced proliferative cells with morphological and gene expression similarities to ESCs.

We previously demonstrated that treatment with the nucleotide derivative BrdU allows for transdifferentiation,[13] and other groups have demonstrated that fusion of stem cells and somatic cells can alter cell properties.[34, 37, 38, 71] In the current study, we show that HMSCs can be dedifferentiated by gene delivery of only nanog, although other factors already present in the cells may contribute to forming ESC-like cells. Recently, delivery of four factors induced pluripotency in mouse fibroblasts. Their use of transcription factors Oct-4, Sox-2, and KLF4 along with the oncogene cMyc was sufficient to induce pluripotent transformation.[72-75] These results have been independently achieved by different labs using human cells with the same set of genes[76-78] or with a combination of nanog, Oct-4, Sox-2, and Lin28.[79]

We found levels of Oct-4, Sox-2 and other genes related to pluripotency and self-renewal were significantly increased after nanog over-expression. Previous reports failed to show formation of ESC-like cells using

any single ESC gene when delivered to stem cells or fibroblasts,[80, 81] nor by combining Oct-4, Sox-2, Klf4 and Myc in adult HMSCs.[77] The use of additional vectors encoding for the simian virus large T antigen (SV40T) and the catalytic subunit for telomerase (hTERT) were able to produce a few colonies but still showed cellular loss with expansion.[77]

The difficulty in converting HMSCs is likely the result of a number of critical factors. First, mesenchymal stem cells have a limited capacity for expansion and vary in their ability to proliferate and differentiate, qualities that decrease with age and vary among sources. They are sensitive to culturing conditions, particularly plating density, supplements and serum quality.[82-85] Gene delivery experiments are also challenging in these cell types given their difficulty to transfect, death from toxicity,[86-89] their propensity to undergo senescence after several passages,[69, 90, 91] or toxicity associated with viral transductions.[89, 92] Additionally, heterogenetity within HMSCs and variation between cultures may account for conflicting results. Research with HMSCs has often produced conflicting results, especially when examining proliferation and stem cell markers.

Previous studies are inconsistent regarding the expression of embryonic stem cell transcription factors Nanog, Oct-4, and Sox-2 in adult stem cells. Oct-4 is present at low levels in HMSC in vitro cultures or can be induced in a subtype of cells using various culture conditions.[30, 84, 93, 94] However, low levels sox2 and nanog are detected in some, but not all HMSCs.[67, 84, 95-97] This inconsistency extends to telomerase activity and the ability to immortalize HMSCs.

Similar to genes associated with pluripotency, telomerase activity has been detected in MSCs by some groups,[98, 99] but not by others.[69, 70, 100-102] Conflicting results are also observed when groups have attempted to immortalize HMSCs through viral delivery of telomerase. Overexpression of telomerase appears to overcome early senescence and generate immortalized cell lines[103-106] while other groups report hTERT alone is insufficient.[100, 101] Alternatively, only a subpopulation of HMSCs may be dedifferentiated by nanog. Presumably cells that endogenously express other necessary stem cell genes would undergo dedifferentiation. This hypothesis is supported by the ability to convert neural stem cells, which already express many stem cell factors including Sox2 and cMyc, to pluripotent cells through forced expression of two factors, Oct-4 and Klf-4,[107] or just Oct-4 alone.[108-110]

In addition to the presence of critical stem cell genes, the level of expression is likely to be imperative in determining cell conversion. Since the combination of Oct-4 and Sox-2, which up-regulates nanog, failed to convert the adult cells to ESC-like cells,[59, 60] high levels of nanog may be the critical factor. Other research found that selection of the cells expressing high levels of nanog after transfection with combination of Oct-4 and Sox-2 has yielded ESC-like colonies.[74]

We observed that the number of ESC-like cell colonies that formed after nanog transfection did not directly correspond to the number of cells receiving the gene. This may be due to the heterogenous population of HMSCs, which varyingly express other factors required to produce ESC-like

cells. Passage number of HMSCs may contribute to variability in results, because changes to HMSCs' ability to differentiate and rate of proliferation are evident by passage six.[90] Continuous passage of cells produces alterations and cell senescence, the proliferative limit of which is commonly referred to as Hayflick's limit.[90, 91]

Cells receiving a non-viral transfection of nanog tended to lose proliferative capability while lentiviral-transfected nanog cells can be maintained over forty passages. HMSCs show extremely low rates of stable transfection using non-viral tranfection.[87] Thus, differences between cells receiving nanog through chemical transfection compared to those receiving it through viral delivery might explain the lack of stable expression of nanog in the non-viral transfected cells. However, sustained nanog expression alone will unlikely induce embryonic stem cell properties in most HMSCs, but will increase their rate of proliferation.

This result, and experiments that demonstrate Oct-4 functions in a similar manner in both HMSCs and ESCs, suggests both cell types share similar regulatory mechanisms. Additionally, embryonic stem cells that have been committed to a mesoderm lineage can be dedifferentiated by forced expression of nanog. We maintain that nanog acts synergistically with other stem cell factors to facilitate dedifferentiation. This work demonstrates the ability of forced expression of nanog to interact with endogenous factors to induce dedifferentiation and expand developmental potential of cells.

This method may be advantageous in developing neural cells without the generation of tetraploid hybrids or ESCs. The ability to generate human

neural cells from adult stem cells allow for the advancement of replacement therapies for neurodegenerative diseases. Still, consideration must be given to how transplanted cells behave under AD-pathological conditions. We observed both glial and neuronal differentiation in aged wild-type mice, but it is uncertain whether this will translate to efficient neuronal differentiation in a disease model.[111, 112] Our previous work has suggested that stem cells will have impaired neuronal differentiation following transplantation into an AD model animal, which shows elevated levels of amyloid β precursor protein (AβPP).[113]

A closer examination in vitro demonstrated the dose-related effects of AβPP in regulating glial differentiation.[114] Recently, our lab has also demonstrated that neuronal differentiation can be achieved by lowering levels of AβPP in the brain using (+)-phenserine.[115] Technology such as this allows both for adult cells to be used in cell replacement therapies for a variety of diseases and also for the ability to create disease-specific cell lines from patients that can be used for research and development of personalized drugs. Although a cure for AD may not be immediate, our results may move us closer toward that goal.

Acknowledgement

This research was supported by NIH grant R01 AG 23472-01. We would like to thank Dr. Austin Smith, University of Cambridge, England, for

nanog clone and Drs. Didier Trono and Patrick Salmon, LVPU, Centre Médical Universitaire, Switzerland, for pLox lentivirus vector. We would like to thank Ms. Stephanie Merchant for providing lab assistance and the manuscript preparation.

CHAPTER TWO:
EMBRYONIC STEM CELL MARKERS DISTINGUISH CANCER STEM CELLS FROM NORMAL HUMAN NEURONAL STEM CELL POPULATIONS IN MALIGNANT GLIOMA PATIENTS

Rationale

The signalling pathways that regulate stem cell self-renewal and pluripotency are likely to have significant implications to cancer research for several reasons. Transplantation of embryonic stem cells form taratomas when transplanted but differentiated cells do not. Induced-pluripotent cells also have the capacity for tumorigenic transformation and forced expression of the gene c-Myc, a gene critical for stem cell proliferation, facilitates transformation of astrocytes to generate tumors with an undifferentiated phenotype.[116] Our previous study has demonstrated the critical role of nanog to expand the developmental potential of human mesenchymal stem cells to pluripotent cells capable of neural differentiation. In this study, we examine the role of embryonic stem cell genes in tumor-derived stem cells and posit that their differential expression in cancer stem cells make them attractive diagnostic and therapeutic markers.

Chapter Summary

Glioblastoma multiforme tumors contain a sub-population of cancer stem cells that contribute to malignancy and resistance to therapy. Previous

studies have characterized these cells based on their similarity to adult neural stem cells and their expression of CD133. In this study, we separated cancer stem cells from non-pluripotent cells comprising the bulk of the tumor based on their respective physical growth properties using both serum and serum-free cell culture media. We successfully generated cancer stem cells from multiple tumor masses as well as from the surgical aspirate. Cancer stem cells were able to proliferate as non-adherent spheroids and differentiated along neuronal and glial lineages following culture in serum-supplemented media. Compared to adherent cancer cells and human fetal neural stem cells served as control, tumor spheroids showed increased rates of proliferation, as measured by BrdU incorporation, and greater resistance to differentiation, respectively. Further characterization of these cells was carried out using immunohistochemistry and real-time PCR to reveal previously undefined molecular markers enriched in cancer stem cells that are absent in both cells comprising the bulk of the tumor as well as in normal neural stem cells. These same markers are down-regulated following differentiation and may serve as important diagnostic and prognostic factors. Moreover, the presence of these unique markers may potentially become targets for future directed therapies.

Introduction

Glioblastoma Multiforme (GBM) is the most common and the most aggressive type of brain tumor, responsible for 18.5% of all primary CNS

tumors. Treatment of these tumors remains a difficult clinical challenge and requires a multimodal approach.[117] Despite obvious benefits, surgery alone or in combination with radiation therapy does not provide prolonged remissions, yielding median survivals of 20 and 36 weeks, respectively, for GBM patients.[118-121] Median survival times may be increased to up to nearly 15 months if over 98% of the tumor is removed[122] or if chemotherapy is integrated with surgery and radiation[123, 124]. Standard chemotherapy plus fractionated radiation therapy and surgery yields a median survival between 50-60 weeks.[123, 124] Unfortunately, there has been little improvement in survival relative to the original documented average span of 44-52 weeks over 80 years ago[125]. The presence of a blood brain barrier[126, 127] and the remarkable degree of molecular heterogeneity within malignant glial cells[128-130] limits the therapeutic effect of chemotherapy and makes patient prognosis poor and recurrence rates reach close to 100%.

The heterogeneity of these GBM tumors, and particularly the presence of a subpopulation of cancer stem cells (CSCs) within them, is believed to be critical to the tumorigenic process.[131-136] Previous studies have suggested that these CSC cells, identified as being positive for the surface marker CD133, within GBM tumors are able to give rise to new tumors following transplantation into nude mice.[131, 134-137] Interestingly, transplantation of CD133 negative cancer cells does not appear to form tumors upon transplantation. CD133 positive cancer stem cells have been compared to human neural stem cells both on growth properties and gene expression.[131, 134, 135] However, many of these comparative studies have been carried out

using fetal neural stem cells rather than endogenous adult neural stem cells.[138] All studies that cite CD133 positivity to be an adult neural stem cell marker reference research on fetal or embryonic stem cell-derived neural stem cells.[139-142] This distinction may be important because non-fetal adult neural stem cells, at least in the subventricular zone, do not express CD133 and have not been as well characterized.[143]

Previous comparative studies of malignant glioma tumor cell heterogeneity fail to provide valuable information as to the similarity of cancer stem cells to adult neural stem cells. Many studies have cited CD133 positivity to be a CSC cell marker even though CD133 positivity has also been established as a marker for normal neural stem cells (NSCs).[137, 138, 140, 141] Thus, the use of CD133 as a surrogate marker to identify tumor stem cells within a GBM may not be clinically useful as glioblastomas contain both differentiated cancer cells and cancer stem cells in addition to normal adult neural stem cells that migrate into the tumor.[144-146] Both NSCs and glial progenitor cells have been found throughout the healthy normal adult brain.[147-154] Neural stem cells travel with tumor cells migrating through the parenchyma of the CNS.[144] In fact, NSCs appear in the area adjacent to glioma implants five days after injection in mice.[146] This migratory phenomenon, which is also observed in brain injury[155], has been proposed as a means of anti-cancer gene delivery.[156, 157] If stem cells are to be a viable vehicle for tumor therapies, then more detailed identification is needed to prevent the accidental implantation of cancer stem cells. Thus, identifying a specific CSC marker to distinguish neoplastic stem cells from non-cancerous

NSCs is crucial for not only understanding the biology of tumor stem cells but also development of effective therapies for GBM.

The ability of CSCs to undergo tumorigenesis, combined with their resistance to chemo- and radiation- therapies,[158-160] is of particular clinical importance given the propensity of gliomas to reemerge following surgery and therapy. As a result, CSC cells may represent a primary therapeutic target in order to achieve complete eradication of the tumor. Although CD133 positive CSCs have been compared to human NSCs both on growth properties and gene expression[131, 134, 135], definitive CSC-specific markers, which relates to tumor stem cell biology have not been found. To help address this problem, this study aimed to characterize different cell populations based on growth properties and to show a distinct population of cells with cancer stem cell properties based on specific cell marker expression patterns.

Materials and Methods

Cell Culture and Isolation

Human glioblastoma tumor masses were removed from patients undergoing craniotomy for primary resection of newly diagnosed tumor identified by magnetic resonance imaging (MRI). All patients provided IRB approved informed consent for the study pre-operatively. Surgically removed tumor specimens were washed, minced, dissociated, and then placed, within

an hour of surgery, inside a 75cm2 flask containing re-suspension medium of DMEM/ F12 supplemented with 10% fetal bovine serum. Following an initial expansion in a monolayer, the tumor cells were switched to a defined serum-free NSC media consisting of DMEM/F12 supplemented with 20ng/ml of basic fibroblast growth factor (FGF-2) and 20ng/ml of epidermal growth factor (EGF) to generate neural sphere formation at different time points. Specifically, cells were placed directly in neural stem cell media or switched at 24, 48, or 72 hours. This culturing system generated cells with two distinct growth properties, adherent cells and floating sphere-forming cells. Adherent cells are likely differentiated tumor cells with limited proliferative potential. Floating neural spheres contain multipotent stem cells. Cells were analyzed using quantitative real-time PCR for expression of embryonic stem cell genes, stem cell transcription factors, and telomerase. Additional characterization included differentiation in media without growth factors such as FGF and EGF and supplemented with fetal bovine serum and immunohistochemical analysis for multiple protein markers.

RNA Isolation and Quantitative Real-Time PCR

Cell culture media was removed from cells and total RNA was extracted from cells using Trizol Reagent (Invitrogen) in accordance with the manufacturer's protocol. Briefly, cells were spun down in a centrifuge tube at low speed to pellet. Media was removed and 1ml of Trizol was added to the

cells and incubated at room temperature for five minutes. After five minutes, 0.2 ml of chloroform per 1ml of Trizol was added to the tubes. The tubes were shaken vigorously for 15 seconds and incubated at room temperature for two minutes. Tubes were then centrifuged at 12,000 x g for 15 minutes at 4˚C. Next, the aqueous phase of the samples was removed and transferred into a fresh tube. To precipitate the RNA, 0.5 ml of isopropyl alcohol was added to each tube and the tube was lightly mixed back and forth for 15 seconds. Samples were then incubated at room temperature for 10 minutes and centrifuged at 12,000 x g for 10 minutes at 4˚C. The supernatant was removes and the RNA pellet was washed once with 1 ml of 75% ethanol per 1 ml of Trizol. Samples were mixed by vortexing and centrifuged at 7,500 x g for five minutes at 4˚C. The supernatant was carefully removed and the RNA pellet was air dried for approximately 10 minutes. The RNA pellet was then resuspended in 100 µl of microbiology grade water and tubes were incubated for 10 minutes at 55˚C. RNA concentration was measured using spectrophotometry. A 1:50 dilution was created using water and absorption readings were taken at 260nm (correlating to RNA concentrations) and 280nm (the ratio of A260/A280 relating to RNA purity). The spectrophotometer was calibrated using cuvettes containing only water.

cDNA synthesis

RNA was reverse transcribed for RT-PCR using iScript cDNA Synthesis Kit (Biorad) to form cDNA. The cDNA reaction took place under the following conditions: 25˚C for 5 minutes, 42˚C for 30 minutes, 85˚C for 5 minutes, and held at 4˚C.

Real-Time PCR

Gene expression was measured by quantitative real-time PCR (qRT-PCR) using gene specific primers. Real-Time PCR was performed using the MyiQ SuperCycler Real Time PCR Detector System (Biorad) using iQ Supermix with SYBR Green (Biorad) for detection. Each reaction tube contained, 12.5 µl of SYBR Green, 8 µl of microbiology grade water, 1 µl of forward primer, 1µl of reverse primer, and 2.5 µl of cDNA, for a total reaction volume of 25 µL. Primers used for real time PCR were: TERT, F 5'-CGGAAGAGTGTCTGGAGCAA-3', R 5'-GGATGAAGCGGAGTCTGGA-3'; CD133, F 5'-CAGAGTACAACGCCAAACCA-3', R 5'-AAATCACGATGAGGGTCAGC-3',

Nanog F 5'-ACAACTGGCCGAAGAATAGC-3', R-AGTGTTCCAGGAGTGGTTGC-3'; Sox2, F 5'-CGGTACCCGGGGATCCCCGCATGTACAACATGATGG-3', R 5'-CATAATGGCCGTCGACCACATGTGTGAGAGGGGCA-3'; Oct4 F 5'-

ATAGACCGGTAATGGCGGGACACCTGGC-3', R 5'-

CATAATGGCCGTCGACCAGTTTGAATGCATGGGAGA-3'; b-Actin, F 5'-CTCTTCCAGCCTTCCTTCCT-3', R 5'-AGCACTGTGTTGGCGTACAG-3'. The Real-Time PCR reaction consisted of Cycle 1: 1 repeat at 94˚C for 5 minutes, Cycle 2: 45 repeats of step 1 at 94˚C for 30 seconds, step 2 at a gradient from 56.2-61.0˚C for 30 seconds, and step 3 at 72˚C for 45 seconds, Cycle 3: 1 repeat at 72˚C for 5 minutes, Cycle 4: 1 repeat at 90˚C for 1 minute, Cycle 5: 90 repeats at 50˚C for 10 seconds with an increase in temperature of 0.5˚C after each cycle starting with cycle 2, and Cycle 6: 1 repeat at 25˚C for 5 minutes. Data collection was enabled at the end of Cycle 2 and melting curve data collection was enabled at Cycle 5.

Immunocytotochemistry

Immunocytotochemical staining was performed using a primary and fluorescent-conjugated secondary antibody protocol. Briefly, cultured cells were washed in phosphate buffered saline (PBS) and fixed in a 4% paraformaldehyde fixative solution for 20 minutes at room temperature. When staining for BrdU incorporation, samples were treated with 2N hydrochloric acid for 20 minutes then washed three times with PBS.

Samples were then incubated at room temperature in a blocking solution of PBS supplemented with 5% donkey serum and 0.2% triton X for one hour. Sections were subsequently transferred to a blocking solution

containing the primary antibodies and incubated overnight at 4˚C. Primary antibodies for the following targets were used: Nanog, Oct4, Sox2, BrdU, BetaIII-tubulin, and GFAP. The following morning, sections were then washed and incubated in a fluorescent-conjugated secondary antibody (1:500 dilution) for 2 hours in the dark, at room temperature. Stained sections were then washed three times with PBS and mounted on a glass slide using a mounting medium containing DAPI to label the nuclei of the cells.

Results

Cells were isolated from either bulk tumor masses or a flush solution of surgical aspirate fluid. Tissue culture isolation of GBM patient brain tissue using a defined serum-free NSC media identified two general groups of cells that form from these tissues. The first group consisted of non-adherent spheroid-forming cells, while the second group consisted of cells forming a monolayer in culture (Figure 7).

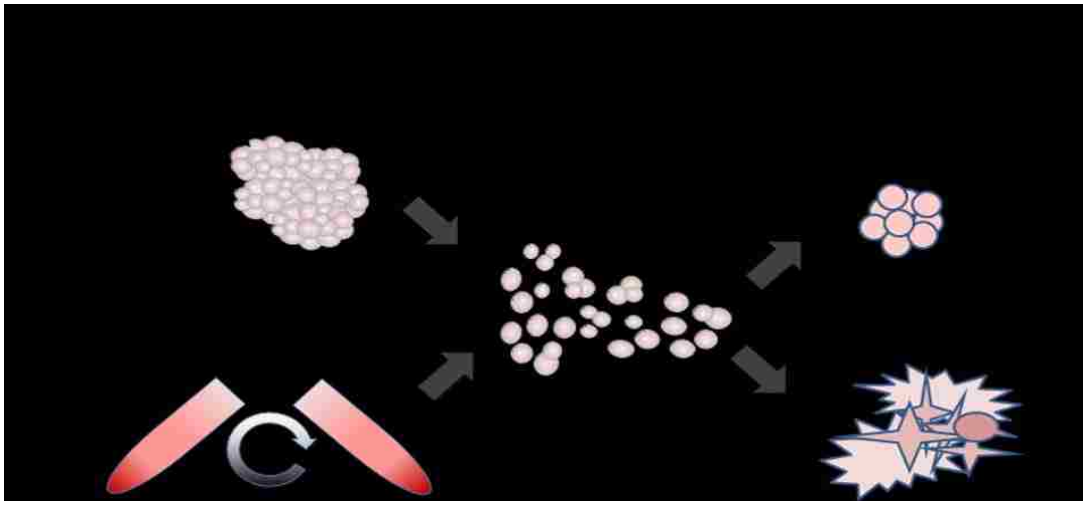

Figure 7: Isolation of cell populations from patient tumor samples. Cells are isolated from patient samples either by dissociating the bulk tumor mass using surgical scalpels (a) or through centrifugation of the surgical aspirate solution (b). Cells isolated from either approach produce populations of cells that are adherent or form floating spheroids. The spheroids have the properties of cancer stem cells while the adherent cells resemble the characteristics of differentiated cells.

Adherent cells were more heterogenous and had lower rates of proliferation. Cells were treated with BrdU for 48 hours to measure proliferation rates and stained using antibodies specific for either CD133 or BrdU. Changes in morphology and the frequency of BrdU-positive cells were observed between the spheroid and adherent cell cultures. Moreover, CD133 expression could be observed in both the spheroid-forming cells, even after 4 days in serum-differentiation media, as well as in some adherent populations (Figure 8).

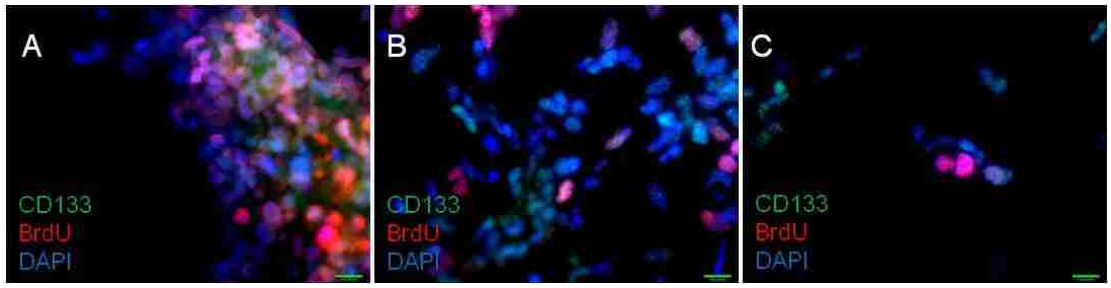

Figure 8: Expression of CD133 and BrdU staining between adherent and floating stem cell cultures. Cells expanded and spheroids had higher BrdU staining and enriched CD133 staining within the spheroid (A). Transferring cells to differentiation media supplemented with 10% FBS for four days reduced the frequency of BrdU-positive cells, but CD133 was still expressed in some of the cells. (B) Although most adherent cells did not express CD133, some positive cells could still be observed (C). Scale bar = 63µm.

Analysis of proliferation rates between patient tumor-derived cell lines revealed distinct differences in proliferation rates, as determined by BrdU-incorporation. Cells expanding as tumor spheroids had significantly higher rates of proliferation compared to adherent lines or tumor spheroids placed in differentiation media. (Figure 9) In fact, following just four days in serum-

supplemented media, proliferation rates in cancer stem cells were reduced by half ($p<0.001$).

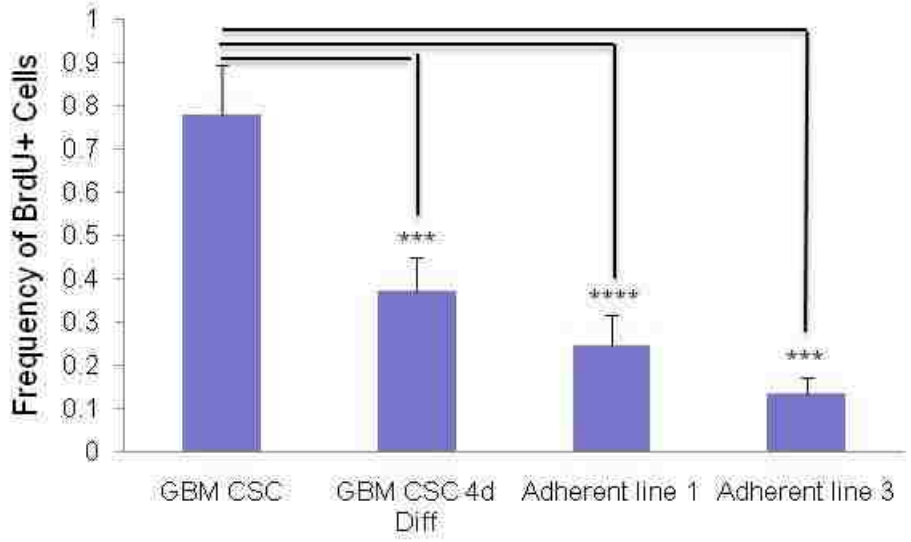

Figure 9: Proliferation rates measured by 48 hour BrdU-treatment Transferring cancer stem cells in serum-supplemented media reduced the rates of proliferation by 50% ($p<0.001$). After 48 hours, only 25% of adherent line 1 and 13% of adherent line 3 were positive for BrdU compared to nearly 80% of cancer spheroids ($p<0.0001$).

Immunohistochemical staining also revealed differences between the floating spheroid cultures, enriched for cancer stem cells, and the adherent cell cultures. Spheroid cultures had a low frequency of expressing markers for neuronal and astrocytic differentiation, as indicating with immunostaining for βIII-tubulin and GFAP, respectively. However, neural spheres derived from the primary tumors were enriched for neural stem cell markers, including Sox2 and Nestin (Figure 10).

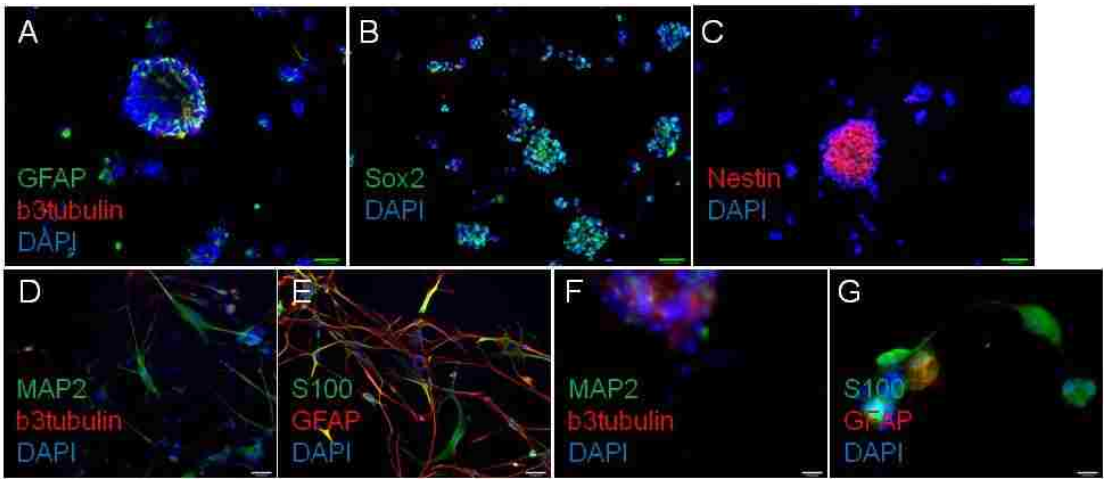

Figure 10: Expression of stem cell and differentiation markers in tumor-derived stem cells. Tumor-derived cells grow as non-adherent spheroids display low rates of GFAP and βIII-tubulin expression (A). Tumor spheroids do readily express stem cell markers Sox2 (B) and Nestin (C). Adherent cell cultures show stronger staining for neuronal differentiation markers (MAP2 and βIII-tubulin, D) as well as astrocytic markers (S100 and GFAP, E). Cancer stem cells could be induced to express both neuronal (F) and astrocytic (G) markers following one-week differentiation in media supplemented with retinoic acid. Scale bar = 63μm.

Alternatively, adherent cell cultures displayed stronger staining for both neuronal (βIII-tubulin and MAP2) as well as astrocytic (S100 and GFAP) markers. The expression of these markers could be up-regulated following one-week differentiation in media without EGF or FGF and supplemented with retinoic acid.

The expression of neural stem cell markers by glioma-derived cancer stem cells has been previously reported. However, we then tested if glioma-derived cancer stem cells express embryonic stem cell markers. Using stem cell gene specific primers, we compared the expression of embryonic stem cell markers nanog, sox2, oct4, and telomerase reverse transcriptase (TERT)

of cancer stem cells to the adherent non-stem cell cultures and normalized gene expression to beta actin (Table 1).

Table 1
PCR Analysis of Clones Resistant to Differentiation Relative to Normal Tumor Non-neurosphere Cells

	Relative gene expression
Nanog	142.51797
Sox2	25.0198286
Oct4	2,069.40456
Tert	11.7533491
B-Actin	1

Note. Gene expression levels are normalized against beta-Actin gene expression level.

In order to investigate the specificity of nanog as a cancer stem cell marker, we compared the expression of nanog from multiple experiments to the gene expression level of nanog from fetal-derived neural stem cells. We found that cancer spheroids have elevated expression of nanog relative to fetal neural stem cells (Table 2).

Table 2
Nanog CT Values for GBM Tumor Clones

RT-PCR experiment	CT value
80616	22.1433
80229	22.8033
80802	23.09
80808	24.6133
80301	25.5267
80709	25.99
80517	27..603333
80821	27.366667
Fetal human NS cell	27.73333

Note. Fetal-derived neural stem cells have relatively lower nanog expression then culture of spheroids derived from glioma tumors, as determined by Ct threshold values.

Although tumor-derived stem cells typically had higher nanog expression, indicated by lower Ct values, the values varied between samples. This reflects the heterogeneity of initial stem cell cultures and the need to establish clonal-derived cell lines. Moreover, it suggests that within the tumor mass, subpopulations of non-cancerous neural stem cells reside and can be isolated.

We then carried out immunohistochemical staining to demonstrate that the up-regulation of gene expression translates to strong protein staining. We demonstrated the cancer stem cells stain positive for antibodies against Nanog, Oct4, SSEA4 and CD133 (Figure 11).

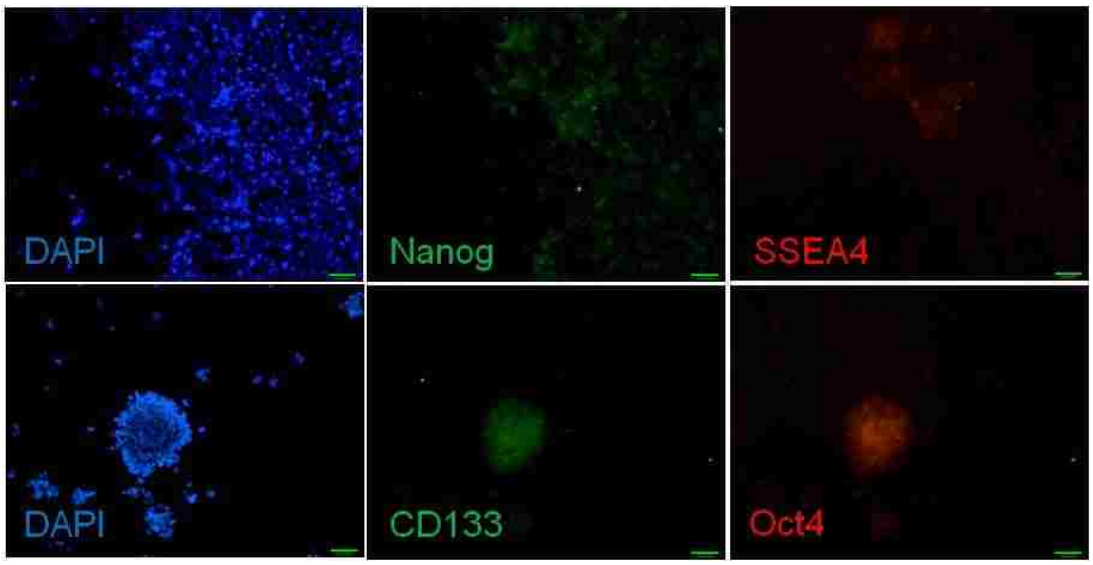

Figure 11: Expression of embryonic stem cell markers in cancer spheroids. Sphere forming cells express embryonic stem cell markers Nanog, SSEA4, Oct4 and CD133.

The expression of embryonic stem cell markers in glioma stem cells provides an important differential marker that can serve to distinguish cancer stem cells from non-cancerous neural stem cells.

Discussion

We were able to demonstrate that despite the heterogeneity of tumor-derived cell lines, distinct populations of cells can be derived based on growth properties. Specifically, cancer stem cells show greater proliferation and express a unique set of markers that are not highly enriched in the adherent cells comprised of cell from the bulk of the tumor. However, tumor stem cell lines derived had varying levels of embryonic stem cell markers. Gene expression analysis revealed tumor spheroids had significantly higher levels of embryonic stem cell genes including Nanog, Oct4, and Sox2. Although Sox2 is required for neural stem cell maintenance, the expression of Nanog and Oct4 was unexpected since previous reports suggest they are not expressed in human neural stem cells. Of the two cell types within the tumor spheroids, those resistant to differentiation had much higher levels of Nanog expression than those that proceeded to differentiate into neural and astroglial lines. This suggests that the high expressing Nanog cells may represent true CSCs while cells that express nanog at low concentrations, if at all, may be infiltrating normal CSCs that migrate to the tumor tissue.

Conclusions

The characterization of cancer stem cells is important from a therapeutic and diagnostic standpoint. The ability of identify unique markers that are enriched in cancer stem cells will lead to novel therapeutic targets. Also, given the role of cancer stem cells in drug resistance and malignancy, these markers may serve as diagnostic markers that can provide insight into the best treatment options for the patient. However, the similarity between brain tumor cancer stem cells and normal endogenous neural stem cells poses a challenge. Elimination of endogenous neural stem cells may contribute to post-chemotherapy cognitive impairment[161, 162] and the use of neural stem cells and vehicles for anti-tumor therapies[144, 145, 156] requires quality control measures to insure transplanted cells have not been transformed during expansion.[163] Given that populations of neural stem cells and cancer stem cells grow as non-adherent tumor spheroids and express CD133, neither is a reliable way to differentiate tumor from non-tumor stem cells within a GBM tumor. Our results suggest that the tumor spheroids derived from GBM brain tissue do contain different stem cell populations, which can be distinguished by the level of embryonic stem cell gene expression. Nanog , a transcription factor critically involved with self-renewal of undifferentiated stem cells seems to be the most differentially expressed in these glioma stem cells. It's levels in normal NS cells and differentiated tumor cells are negligible. From our results, it seems that Nanog might be a better CSC marker than the previously described CD133. Nanog, is thought to play

a key role in maintaining pluripotency. Loss of Nanog function causes differentiation of embryonic stem cells into other cell types and Nanog over-expression enables stem cell propagation for multiple passages during which they remain pluripotent. Interestingly, p53 binds to Nanog's promoter and suppresses its expression resulting in stem cell differentiation.[164, 165]

Since Nanog is known to prevent differentiation of embryonic stem cells, a similar mechanism may be preventing differentiation of the CSCs. Future research studying Nanog's role in regulating GBM tumor stem cell differentiation and ways to block Nanog's effects on these cells may allow for therapies that enhance our ability to successfully treat patients with GBM tumors.

CHAPTER THREE:
CHARACTERIZATION OF CANCER STEM CELLS WITHIN GLIOBLASTOMAS AND THEIR INHIBITION WITH HISTONE DEACETYLASE INHIBITORS

Rationale

The signalling pathways that regulate stem cell self-renewal and pluripotency are likely to have significant implications to cancer research for several reasons. Transplantation of embryonic stem cells form taratomas when transplanted but differentiated cells do not. Induced pluripotent cells also have the capacity for tumorigenic transformation and forced expression of the gene c-Myc, a gene critical for stem cell proliferation, facilitates transformation of astrocytes to generate tumors with an undifferentiated phenotype.[116] Our previous study has demonstrated the critical role of nanog to expand the developmental potential of human mesenchymal stem cells to pluripotent cells capable of neural differentiation. In this study, we examine the role of embryonic stem cell genes in tumor-derived stem cells and posit that their differential expression in cancer stem cells make them attractive diagnostic and therapeutic markers.

Cancer stem cells are highly tumorigenic and resistant to chemotherapy and radiation. We previously identified to role of embryonic stem cell genes in distinguishing these cancer stem cells, but how these genes are distinguished from cells comprising the bulk of the tumor has not been examined. We hypothesize that these stem cell genes are critical to the

tumorigenic process and their expression correlates with malignancy. Furthermore, we establish a new culturing method of isolating cancer stem cells from the surgical flush and identify histone deacetytase inhibitors as promising therapeutic options to target cancer stem cells.

Chapter Summary

Glioblastoma multiforme tumors are highly malignant brain tumors with limited effective treatment options. Within these tumors, a subpopulation of cancer cells with stem cell properties, have been shown to be extremely resistant to radiation and current chemotherapeutic agents, and have the ability to readily reform tumors. Therefore, the characterization of cancer stem cells and the development of therapeutic agents that effectively target them are extremely important.

In this study, we characterize these so-called cancer stem cells based on gene expression using quantitative real-time PCR and immunohistochemical staining for stem cell markers. We successfully isolated cancer stem cells from both the bulk of the tumor and the surgical aspirate fluid, demonstrating a new isolation technique and showing heterogeneity of stem cells within the tumor. Moreover, we examined the effects of histone deacetylase inhibitors trichostatin A (TSA) and valproic acid (VPA) on the proliferation and gene expression profiles of cancer stem cells.

Cells expanded in stem cell cultures expressed both neural and embryonic stem cell markers Nanog, Oct4, Sox2, SSEA4, and CD133. Gene expression analysis showed significant enrichment of these markers in cancer stem cell cultures relative to cells grown in serum-supplemented media. Transferring cancer stem cells to serum-supplemented media reduced proliferation rates and greatly diminished expression of stem cell markers. The histone deacetylase inhibitors TSA and VPA were effective at inhibiting the proliferation of cells and down-regulating cancer stem cell markers.

This study characterizes the expression of multiple embryonic stem cell markers in glioblastoma-derived stem cell lines. Furthermore, we demonstrate the effectiveness of histone deacetylase inhibitors TSA and VPA at significantly inhibiting cancer stem cell growth and down-regulation of stem cell markers.

Introduction

Glioblastoma multiforme (GBM) tumors are aggressive gliomas that demonstrate strong resistance to currently available chemotherapy options and frequent recurrence following treatment. After diagnosis, median survival times of GBM patients have been reported to be 20 weeks with surgery alone, or up to 36 weeks if combined with radiation therapy.[118-121, 166] Median survival times may be increased to nearly 15 months if either over 98% of the tumor is removed[122] or chemotherapy is integrated with surgery and

radiation treatment.[123, 124, 167] Unfortunately, this offers only a slight improvement relative to the average survival span of 44-52 weeks documented over 80 years ago.[125]

The heterogeneity of these GBM tumors, and particularly the presence of a subpopulation of cancer stem cells within them, is believed to be critical to the tumorigenic process.[131-136] Earlier studies have demonstrated the existence of a subpopulation of cancer stem cells, identified as testing positive for the surface marker CD133, within glioblastoma tumors that are able to give rise to new tumors following transplantation into nude mice.[133-135, 143, 159, 168-170] Cancer cells that are negative for CD133 did not appear to form tumors upon transplantation nor share stem cell characteristics observed in CD133+ cells.[134, 135] These CD133-positive cancer stem cells have been compared to human neural stem cells for both their growth properties and gene expression.[134, 138, 143, 159, 171]

The ability for cancer stem cells to undergo tumorigenesis, in conjunction with the resistance these cells have for radiation and chemotherapy,[160, 172-175] is of particular clinical importance given the propensity of gliomas to re-emerge following treatment. This study characterizes different cell populations based on growth properties and shows the existence of a distinct subpopulation of cells with cancer stem cell properties. We characterize these cells based on their expression of stem cell markers and demonstrate the effectiveness of histone deacetylase inhibitors trichostatin A and valproic acid at inhibiting their growth.

Materials and Methods

Cell Culture and Isolation

Human glioblastoma cells were removed from patients undergoing treatment surgery who have provided informed consent for the study. Surgically removed tumor specimens were washed, minced, dissociated, and then plated inside a 75cm2 tissue culture-treated flask containing re-suspension medium of DMEM/F12 (Invitrogen) supplemented with 10% fetal bovine serum (FBS, Gibco) within an hour of surgery. Following an initial expansion in a monolayer, the tumor cells were switched to a defined serum-free NSC media consisting of DMEM/F12 supplemented with 2% B27 (Gibco), 1% antibiotic/antimycotic (Gibco), 9U/ml of heparin (Sigma), 20ng/ml of basic fibroblast growth factor (FGF-2, R&D Systems) and 20ng/ml of epidermal growth factor (EGF, R&D Systems) to generate neural sphere formation at different time points using non-tissue culture-treated suspension flasks and plates. Specifically, cells were placed directly in neural stem cell media or switched at 24, 48, or 72 hours. This culturing system generated cells with two distinct growth properties, adherent cells and floating sphere-forming cells. Adherent cells are likely differentiated tumor cells with limited proliferative potential, whereas floating neural spheres contain multipotent stem cells. Adherent cells were expanded by enzymatic dissociation (Accumax, Innovative Cell Technologies); suspension cells were dissociated by quarter-sectioning with the razor blade [176] or pelleted and dissociated with 0.5ml of

Accumax and gentle up-and-down pipetting for 5 minutes. Using quantitative real-time PCR, cells were analyzed, for expression of neural stem cell genes, stem cell transcription factors, tumor cell markers, and genes associated with neural and glial differentiation. Additional characterization included differentiation in serum supplemented media and antibody staining with stem cell and neural lineage markers.

Isolation of Cells from Surgical Aspirate

Surgical aspirate samples were collected during routine procedures to remove GBM tumors. The brain tissue was separated from the red blood cells by successive gradient purification (four times) through centrifugation at 300g using DMEM. The red blood cells formed a distinct layer that allowed for easier isolation of cells from the tumor. Cells were then placed in T75 adherent and suspension culture flasks and cultured overnight in DMEM supplemented with 10% FBS and 1% antibiotic/antimycotic. The following day, cell culture media was collected and centrifuged at 200g three times using DMEM to collect the pellet of nucleated cells, while separating out most of the remaining red blood cells. The media was then changed to neural stem cell media to facilitate the generation of spheroids. Once spheroids were generated, they were cultured in suspension flasks to reduce the occurrence of spontaneous differentiation. The adherent cells, when nearing confluence,

were enzymatically-dissociated and expanded into new flasks at a 1:2 dilution in cell culture media.

Culturing of Human Neural Stem Cell Lines

Two different human neural stem cell lines were used to compare growth properties and to serve as a positive control for immunostaining. Fetal-derived human neural progenitor cells (Lonza) were grown in suspension and expanded. Additionally, an adherent immortalized tumor cell line, ReNcell CX (Millipore) was grown in flasks pre-coated with laminin in non-serum stem cell media.[177, 178]

Generation of Clonal-Derived Cancer Stem Cell Lines

To generate clonal-derived cancer stem cell lines, we dissociated cancer spheroids and plated individual cells inside wells of a 96-well plate. Wells that received multiple cells were excluded from further culturing. Individual cells that re-grew colonies were then selected and passaged again in single cell cultures inside a 96-well plate to insure that spheroids were indeed clonally derived. This process was followed for cancer stem cells isolated from both the tumor mass and the surgical aspirate.

RNA Isolation and Quantitative Real-Time PCR

Cell culture media was removed from cells and RNA extraction was performed using a commercially available TRIZOL reagent (Invitrogen). RNA concentrations were measured using spectrophotometry. Gene expression was measured by quantitative real-time PCR (qRT-PCR) using gene specific primers. Primers were designed using commercially available software[179] (Oligo 6.8, Molecular Biology Insights, Cascade, CO) and freely available online programs (Primer3 and Primer3 Plus).[180, 181] Given the high variability of "housekeeping genes," [182-187] we tested multiple housekeeping genes (β-actin, GAPDH, and HPRT) and β-actin showed the least variation in our preliminary testing studies (data not shown). Our optimization results are supported by studies that suggest GAPDH and HPRT activity may be altered in tumors because of mutations, altered regulation or treatments.[182, 186-192] Primers were tested for optimal annealing temperature, efficient application of the target sequence, and single product formation. Primers that formed multiple products-such as primer dimerization-as indicated by melt curve analysis and gel electrophoresis, were not used for qRT-PCR analysis. However, two different sets of nanog primers, spanning different exons, were used to determine if a splice variant was formed. No variant was observed.

Cell Differentiation

Expanded human neural stem cells or tumor-derived spheroids were cultured in serum-free basal media supplemented with a 1% antibiotic/antimycotic solution for one week to assess differentiation.[193] All-trans retinoic acid (Sigma) at a 1μM concentration was supplemented in some cultures to enhance differentiation in serum-free conditions.[194-196] Alternatively, serum-induced differentiation was performed using serum-supplemented (10% FBS) DMEM, each containing 1% antibiotic/antimycotic solution in tissue culture treated plates.

Drug Treatments

Histone deacetylase inhibitors (HDACi) Valproic acid (VPA) and trichostatin-A (TSA) stocks were prepared by dissolving the compounds in ethanol and then diluted to working stocks. The total ethanol concentration treated for cell cultures was less than 0.1% and did not affect cell growth. Control cells consisted of treatment with the same percentage of ethanol.

Immunohistochemical Staining

Immunohistochemical staining was performed using a primary and fluorescent-conjugated secondary antibody protocol. Briefly, cultured cells

were washed in phosphate buffered saline (PBS) and fixed in a 4% paraformaldehyde fixative solution for 20 minutes at room temperature. When staining for BrdU incorporation, samples were treated with 2N hydrochloric acid for 20 minutes then washed three times with PBS. Samples were then incubated at room temperature in a blocking solution of PBS supplemented with 5% donkey serum and 0.2% triton-X for one hour. Sections were subsequently transferred to a blocking solution containing the primary antibodies and incubated overnight at 4°C. Primary antibodies for the following targets were used: Nanog (1:500, Ab9220, Chemicon), Oct4 (1:500, MAB4401, Chemicon), Sox2 (1:500, Ab5603, Chemicon), BrdU (1:200, Ab6328, Abcam), βIII-tubulin (1:1000, T8660 and T2200, Sigma), and GFAP (1:1000, G9269 and G3893, Sigma), CD133 (1:100, Ab16518, Abcam), MAP2 (1:500, Ab5622, Abcam), MCM2 (1:500, Ab6153, Abcam), SSEA4 (1:500, MAB4304, Chemicon), Nestin (1:500, MAB353, Chemicon).

The following morning, sections were then washed and incubated in a fluorescent-conjugated secondary antibody (1:500 dilution) for 2 hours in the dark at room temperature. Stained sections were then washed three times with PBS and mounted on a glass slide using a mounting medium containing DAPI to label the nuclei of the cells.

Microscopy

Cells were analyzed using an inverted Leica microscope with a mounted camera using Openlab 4.0 software (Improvision). Negative controls consisting of fixed cells immunostained without incubation with secondary antibodies were used to rule out auto-fluorescence or non-specific binding. Cell imaging was done using the same camera settings and exposure range for each sample. Images were then saved as TIFF files and combined in Photoshop as RBG images. Multiple samples were photographed and cells were counted and examined. Quantitative analysis of cell numbers was performed by counting of blindly-selected regions in multiple samples using Photoshop.

Statistical Analysis

Data was compiled in Microsoft Excel and GraphPad Prism software and statistical analysis was carried out using a minimum of three independent samples and graphed using the mean and standard deviation. Real-time PCR data was analyzed based on comparison of normalized Ct values. [50, 51, 184, 197] Although previous studies by our lab have relied on visual estimations of relative gene expression[113, 114] or employed a standard t-test for statistical analysis,[198, 199] we employed a t-test for unequal variance. The Student t-test holds true for data that has a normal

distributions,[200, 201] while the test used for these experiments does not assume equal variance.[202, 203] This new approach overcomes problems with the conventional t-test for gene expression analysis[51, 184, 204, 205] and does not require testing for normality,[202, 203] a required step that typically is not carried out. To further validate the appropriateness of this approach, we carried out an F-test demonstrating that our gene expression data does not follow a normal distribution. Cell counting was performed on blindly-selected regions that were photographed from at least three independent wells. Cell count data was analyzed for One-way ANOVA using Bonferroni multiple comparisons post-hoc testing.

Results

Isolation of Cancer Stem Cell Lines

We attempted to generate cancer stem cell and non-stem cell lines from both the mass of the tumor and the surgical flush. Two distinct cell populations were generated from culturing cells in serum-supplemented or serum-free media. Cells cultured in conventional serum-supplemented media adhered to the flask and displayed heterogenic morphology-typically with branched spindle-like processes and high nuclear to cytoplasmic ratios, (Figure 12, A1) which is consistent with observations by multiple groups.[128, 206-209] Contrastingly, when cultured in serum-free conditions, cells grew in

suspension forming spheroids (Figure 12, A2). Although serum-free conditions did exhibit adherent cells, they were relatively non-proliferative, and by the third passage, cultures consisted almost entirely of suspended cells resembling neural stem cell spheroids.(Figure 12) Serum-free culturing conditions and samples that were generated from the surgical flush had significantly more cellular debris compared to serum-supplemented cultures of cells generated from the tumor mass, simply because the floating debris is easily removed when changing the media of adherent cells (Figure 12, A3-4). Floating stem cell cultures required additional low-speed centrifugation to separate the smaller pieces of debris and residual red blood cells.

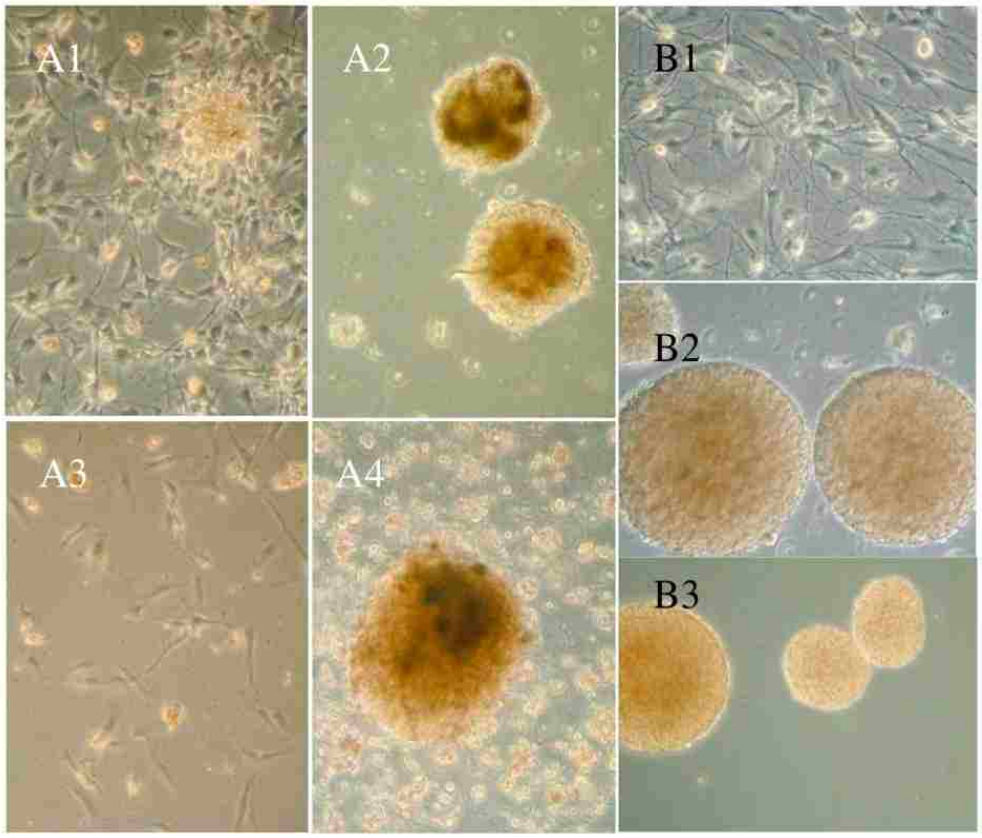

Figure 12: Morphology of cells in culture. Dissociation of tumor tissues can produce two distinct cell populations, adherent cells that grow in a monolayer in serum-supplemented culture (A1) or cells that grow in suspension in NSC culture conditions (A2). Cells isolated from the surgical flush are also give rise to monolayer (A3) and spheroid-growing cells (A4), in serum-supplemented and NSC culture media, respectively. More cellular debris is present with surgical aspirate-derived cultures. Cells grown in serum-supplemented (B1) and serum-free stem cell media (B2) maintain their growth patterns in continuous culture (5 weeks). Tumor-derived cells expanded in serum-free stem cells cultures resemble fetal-derived non-cancerous stem cells (B3). Scale bar = 63µm.

Nonetheless, by two to three weeks, floating spheres were generated from either cell source and were easily expanded by passaging and re-seeding in new suspension flasks. The initial passaging of the cancer stem cells produced floating and adhering cells, suggesting that early passaged cells still contain non-stem cells or are still prone toward spontaneous differentiation. However, after one month of continuous culture, cell cultures were less heterogeneous-with retracted cytoplasmic processes compared to serum-cultured cells-and began to readily expand (Figure 12, B1-2). The stem cell cultures produced proliferating spheroids (Figure 12, B2) that resembled human fetal-derived neural stem cells Figure 12, B3). We also examined slight variations in culturing conditions to determine the optimal approach to generating cancer spheroids. We compared the culturing of cells after immediate plating in stem cell media to transference after 24, 48, and 72 hours from serum-supplemented media.

Surprisingly, initial culturing with only neural stem cell media produced very few viable neural spheres; culturing in serum media for 48 hours also resulted in a limited number of slow proliferating spheres; and, no spheroids were generated in cultures that were initially treated with serum media for 72 hours. Culturing cells in serum media overnight prior to transferring to neural stem cell media yielded the most spheroids. Hence, given the time points tested, the optimal time to transition to neural stem cell media is 24 hours post-plating.

Characterization of Cancer Stem Cell Lines Based on Immunohistochemistry

We compared the expression of multiple stem cell markers among the adherent serum-supplemented cell cultures, the tumor spheroids, and an immortalized neural stem cell line, ReNcell CX. The immortalized neural progenitor cell line ReNcell Cx grows as an attached monolayer in plates pre-coated with laminin. Incubation of fixed samples with only secondary antibodies conjugated with either FITC or TRITC revealed no detectable non-specific binding or auto-fluorescence (Figure 13, A). The immortalized stem cell line shows positive immunostaining for the early neuronal and astrocytic markers βIII-tubulin (Figure 13, B2) and GFAP (Figure 13, B3), respectively. The ReNcell Cx cells were also positive for stem cell markers Nestin (Figure 13, C2),

CD133 (Figure 13, C3), MCM2 (Figure 13, D2), and Sox2 (Figure 13, D3). However, this line showed no appreciable staining for embryonic stem cell markers Oct4 (Figure 13, E2) and Nanog (Figure 13, E3).

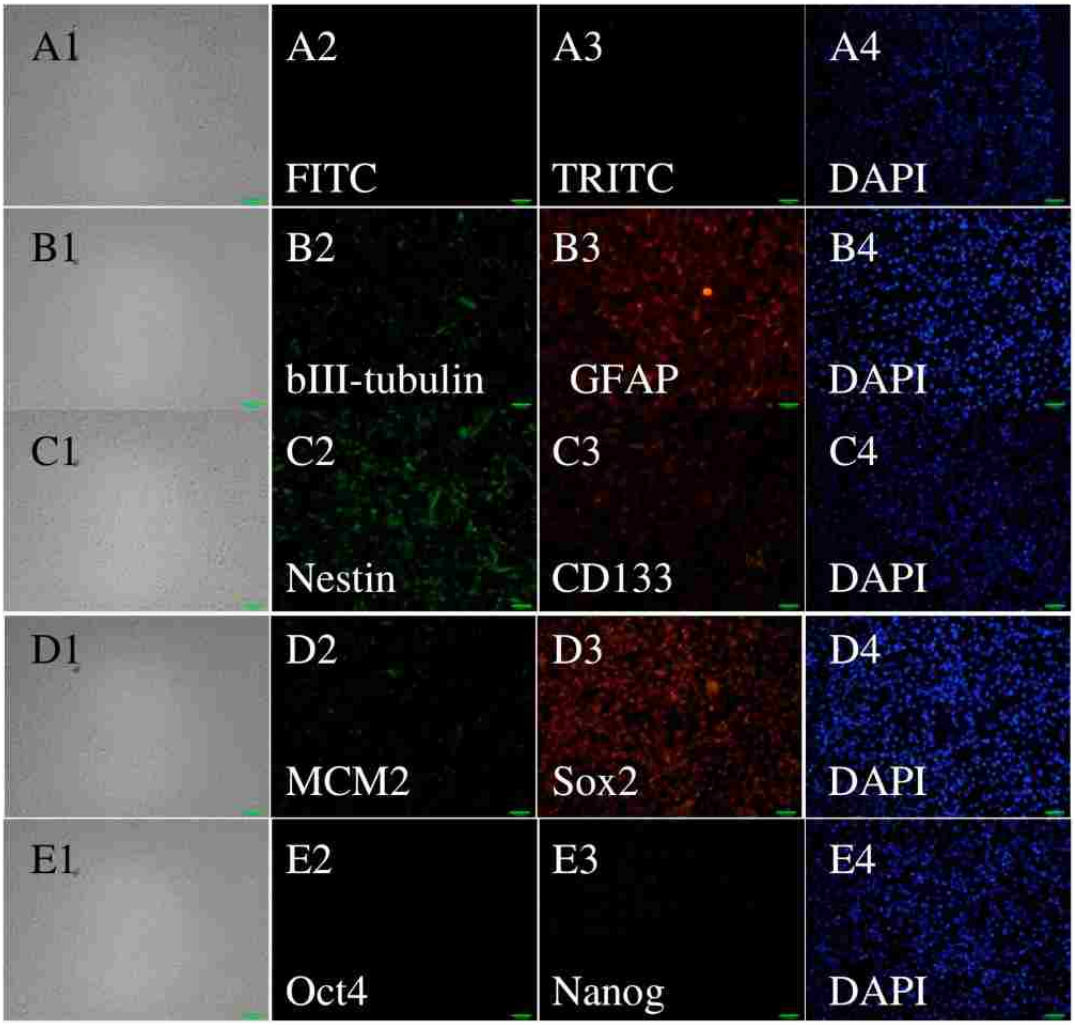

Figure 13: Expression of stem cell and lineage markers in the ReNcell Cx line. The immortalized neural progenitor cell line ReNcell Cx grow as an attached monolayer in plates pre-coated with laminin. Fixed cells were treated with DAPI to stain the nuclei (A-E4). They do not show positive staining when stained with secondary antibodies conjugated with either FITC (A2) or TRITC (A3). They do demonstrate expression of lineage markers βIII-tubulin (B2) and GFAP (B3) as well as neural stem cell markers. ReNcell Cx cells also have positive staining for Nestin (C2), CD133 (C3), MCM2 (D2), and Sox2 (D3). However, the neural stem cell line does not stain positive for the embryonic stem cell markers Oct4 (E2) or Nanog (E3). Scale bar = 63μm.

Adherent tumor-derived cells grown in serum-supplemented media do not appreciably express stem cell markers CD133 (Figure 14, A2) or Oct4 (Figure 14, A3). However, cells do demonstrate strong expression of the mature neuronal marker MAP2 (Figure 14, B2) as well as the early lineage marker βIII-tubulin (Figure 14, B3). The cells also have strong expression of glial differentiation markers S100 (Figure 14, C2) and GFAP (Figure 14, C3). The expression of differentiation markers is consistent with their differentiated spindle morphology.

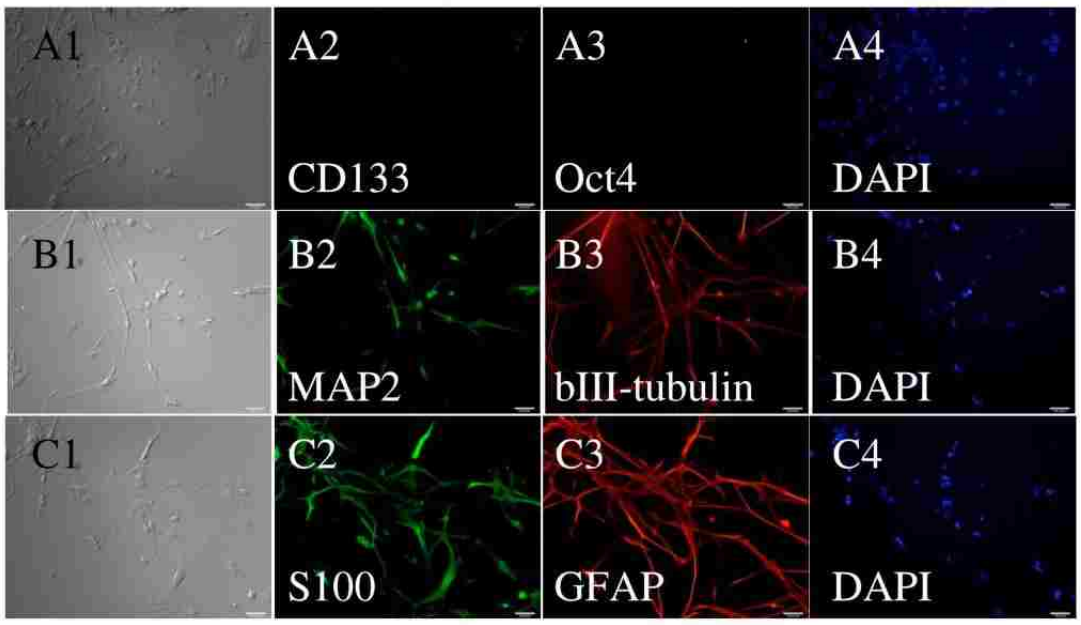

Figure 14: Expression of stem cell and lineage markers in adherent tumor-derived cells. Adherent tumor-derived cells grown in serum-supplemented media do not appreciably express stem cell markers CD133 (A2) or Oct4 (A3). However, cells do demonstrate strong expression of the mature neuronal marker MAP2 (B2) as well as the early lineage marker βIII-tubulin (B3). The cells also have strong expression of glial differentiation markers S100 (C2) and GFAP (C3). Scale bar = 63μm.

Glioma stem cells, expanded in serum-free and growth factor-supplemented stem cell media, did positively stain for neural and embryonic stem cell markers, as well as for markers of differentiation. Tumor spheroids express neural stem cell markers CD133 (Figure 14, A2 and 15, E2), Nestin (Figure 15, B2), transcription factor Sox2 (Figure 15, B3 and 15, D2) and proliferation marker MCM2 (Figure 15, E3). Moreover, the spheroids were also immunopositive for embryonic stem cell markers Nanog (Figure 15, C2), Oct4 (Figure 15, A3), and SSEA4 (Figure 15, C3). However, cells were negative for embryonic stem cell surface marker TRA-1-60 (Figure 15, D3).

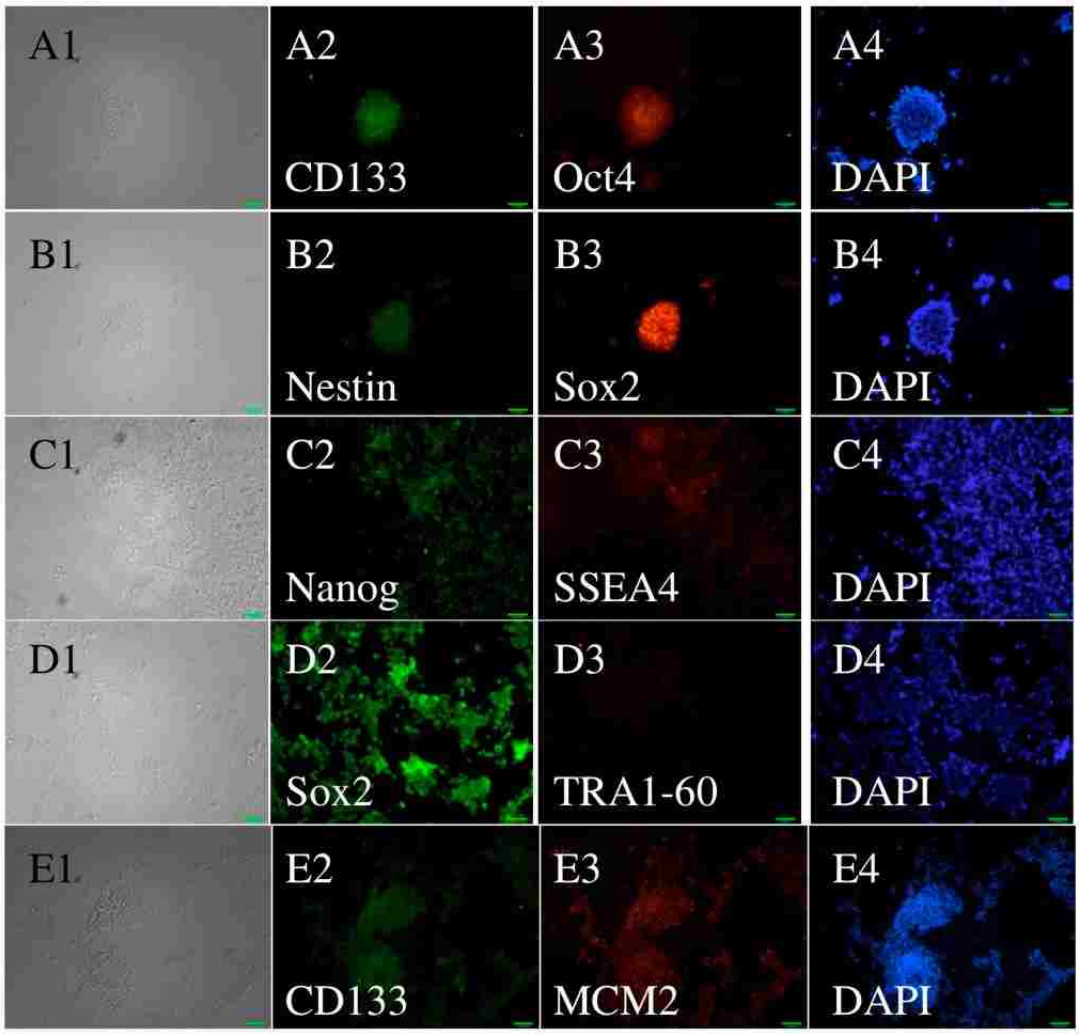

Figure 15: Expression of stem cell markers in tumor-derived stem cells. Tumor-derived cells grow as non-adherent spheroids express stem cell markers CD133 (A2, E2), Oct4 (A3), Nestin (B2), Sox2 (B3, D2), Nanog (C2), SSEA4 (C3) and MCM2 (E3), but not surface marker TRA1-60 (D3). Scale bar = 63μm.

GBM stem cells also expressed low levels of early lineage markers βIII-tubulin (Figure 16, A3 and 16B3) and GFAP (Figure 16, A2 and 16, C3). The tumor-derived stem cells were also weakly positive for differentiation markers MAP2 (Figure 16, B2) and S100 (Figure 16, C2). Although spheroids were comprised of cells that were positive for both neuronal and glial markers, two different lineage markers were typically not expressed within the same cell. We also found cancer stem cells to have higher rates of proliferation relative to serum differentiation-induced cells and adherent non-stem cell cultures. Moreover, when differentiation is induced in the cancer stem cells, we observe the loss of stem cell markers and an increase in markers of differentiation.

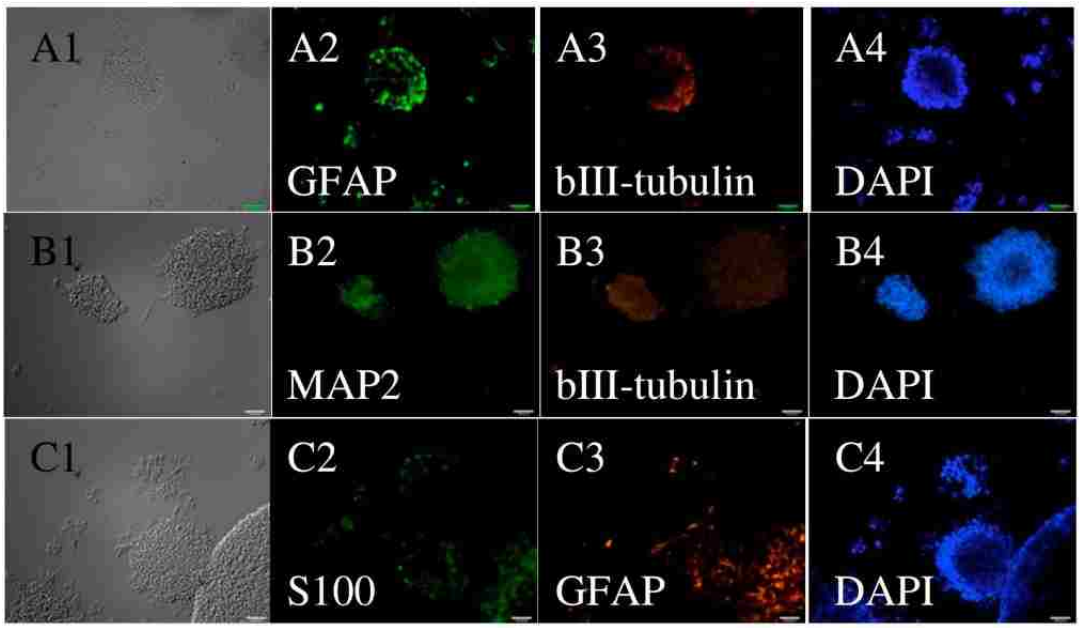

Figure 16: Expression of lineage markers in tumor-derived stem cells. The cells also expressed developmental markers for neuronal (βIII-tubulin (A3) and MAP2 (B2)) and glial (GFAP (A2, C3), S100 (C2)) lineage differentiation. Scale bar = 63μm.

Gene Expression Analysis of Cancer Stem Cell Lines

We next examined the relative differences in gene expression profiles among three different cell lines, two of which were generated from two different sources (tumor mass and surgical flush) from the same patient (AA1-02 and AA1-06). We measured consistently higher expression of genes critical to stem cell proliferation and self-renewal in the glioma stem cells relative to the adherent non-stem cell cultures. Cancer spheroids derived from either the bulk of the tumor tissue (CSC AA1-02 and CSC AA3-01) or the surgical flush (CSC AA1-06) demonstrate enriched expression of stem cell markers and other genes compared to adherent tumor cells expanded in serum-supplemented cultures. Cancer stem cell line AA1-02 showed elevated expression of GAPDH (4.2x, $p<0.01$) and stem cell transcription factors nanog (99.1x, $p<0.0001$), oct4 (9.3x, $p<0.01$), and sox2 (1341x, $p<0.00001$). Cell line CSC AA1-06 has enhanced relative expression of stem cell markers nanog (20.9x, $p<0.0001$) and sox2 (461.2x, $p<0.00001$). Telomerase reverse transcriptase (TERT) and telomeric repeat-binding factor 1 (TERF1) were both significantly higher in both cancer stem cell lines (TERT: 129.0x and 682.1x, $p<0.001$ and $p<0.001$; TERF1: 8.8x and 1.6x, $p=0.01$ and 0.01, respectively).

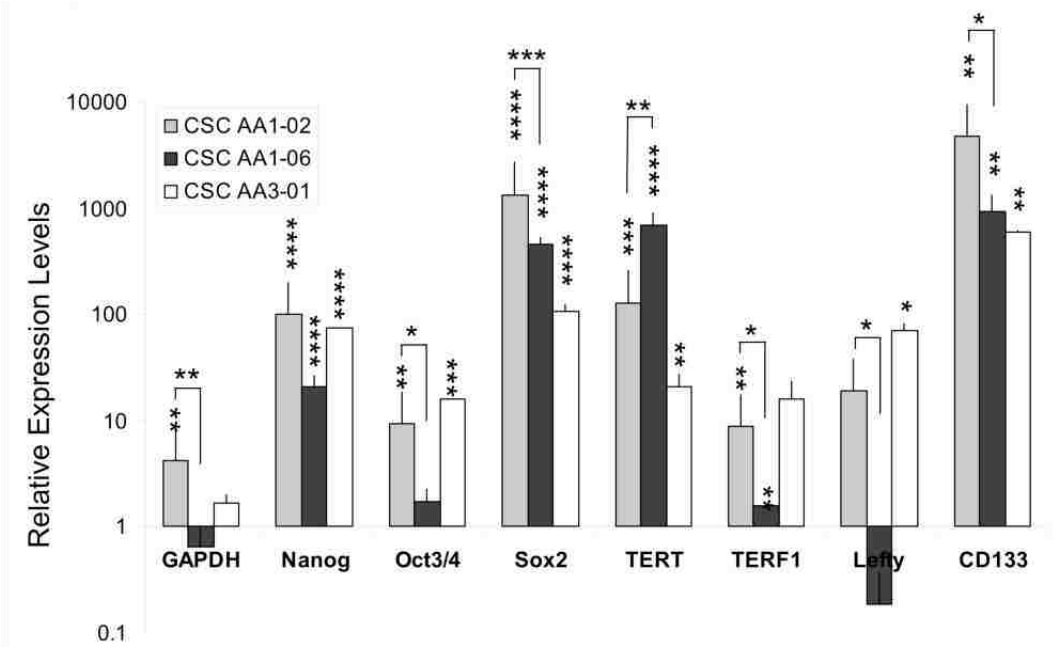

Figure 17: Cancer spheroids have enhanced stem cell gene expression patterns. Cancer spheroids derived from either the bulk of the tumor tissue (CSC AA1-02 and CSC AA3-01) or the surgical flush (CSC AA1-06) demonstrate enriched expression of stem cell markers and other genes compared to adherent tumor cells expanded in serum-supplemented cultures. Cancer stem cell line AA1-02 showed elevated expression of GAPDH and stem cell transcription factors nanog, oct4, and sox2. Cell lines CSC AA1-06 and CSC AA3-01 show enhanced expression of stem cell markers nanog and sox2. Telomerase reverse transcriptase (TERT) and telomeric repeat-binding factor-1 (TERF1) were both significantly higher in the cancer stem cell lines. The stem cell genes that showed the greatest differential expression were the stem cell transcription factors nanog and sox2 along with tert and surface marker CD133. Statistical significance indicated by asterisks: *p<0.05, **=p<0.01, ***p<0.001, ****p<0.0001.

The presence of active telomerase functioning is commonly observed in many tumors, but is extremely low in adult neural stem cells and glioma cells expanded in serum-supplemented cultures. The gene Lefty, which regulates both embryonic stem cell expansion and early neuroectoderm differentiation,[210-213] was not statistically enhanced nor decreased in either the AA1-02 ($p=0.35$) nor the AA1-06 ($p=0.10$) line. However, the surface marker CD133 appears to have the greatest discrepancy in expression between the adherent tumor cells and tumor spheroids in CSC lines AA1-02 (4748.6x, $p<0.01$) and AA1-06 (926.9x, $p<0.01$).

Cancer stem cell line AA3-01 has robust over-expression of the embryonic stem cell transcription factors nanog (74.1x, $p<0.0001$), oct4 (15.8x, $p<0.001$), and sox2 (106.3x, $p<0.0001$) relative to adherent serum-supplemented cell cultures. This cell line also expressed higher levels of tert (21.1x, $p<0.01$), terf1 (16.2x, $p=0.058$), and lefty (71.2x, $p<0.05$). CD133, as expected, had significantly greater relative expression in the AA3-01 line as well (588.4x, $p<0.01$).

The gene expression levels between the tumor mass-derived (AA1-02) and surgical flush-derived (AA1-06) cell lines was significantly different for almost all genes tested. Cell line AA1-02 showed greater relative expression levels of GAPDH ($p<0.01$), oct4 ($p<0.05$), sox2 ($p<0.001$), terf1 ($p<0.05$), lefty ($p<0.05$), and CD133 ($p<0.05$) when compared to the AA1-06 line. Although the relative expression of tert was enhanced in the AA1-06 line ($p=0.01$). Relative expression levels of nanog were not statistically different between the two lines ($p=0.11$).

Differentiation Analysis of Cancer Stem Cell Lines

Cancer stem cells were similar to healthy neural stem cells with respect to morphology, a non-adherent spheroid growth pattern, and the ability to differentiate into neural and glial progenitors, as indicated by βIII-tubulin and GFAP immunostaining. However, cancer stem cells were more resistant to differentiation, particularly when the tumor spheroid was intact. Human fetal-derived neural stem cells underwent differentiation when transferred to a serum-free and non-growth factor-supplemented basal cell culture medium (Figure 18, A). Cells, grown as neural spheres, attached and differentiated along both neuronal (βIII-tubulin, Figure 18, A1) and glial (GFAP, Figure 18, A2) lineages. Following one week of culturing in basal media, neural stem cells developed a differentiated morphology with extensive cellular processes (Figure 18, A). When the cancer spheroids were transferred to serum-free differentiation cultures, the cells attached and displayed enhanced expression of (βIII-tubulin, Figure 18, B1) and glial (GFAP, Figure 18, B2). However, the glioma stem cells were far more resistant to differentiation, particularly when the spheroid remained intact. (Figure 18, B) Serum-free differentiation failed to eliminate the expression of stem cell markers within the spheroid. After one week, cancer stem cells still maintained the expression of CD133 (Figure 18, C1) and Oct4 (Figure 18, C2). The use of retinoic acid, an enhancer of differentiation, was still ineffective at eliminating the expression of stem cell markers (Figure 18, D).

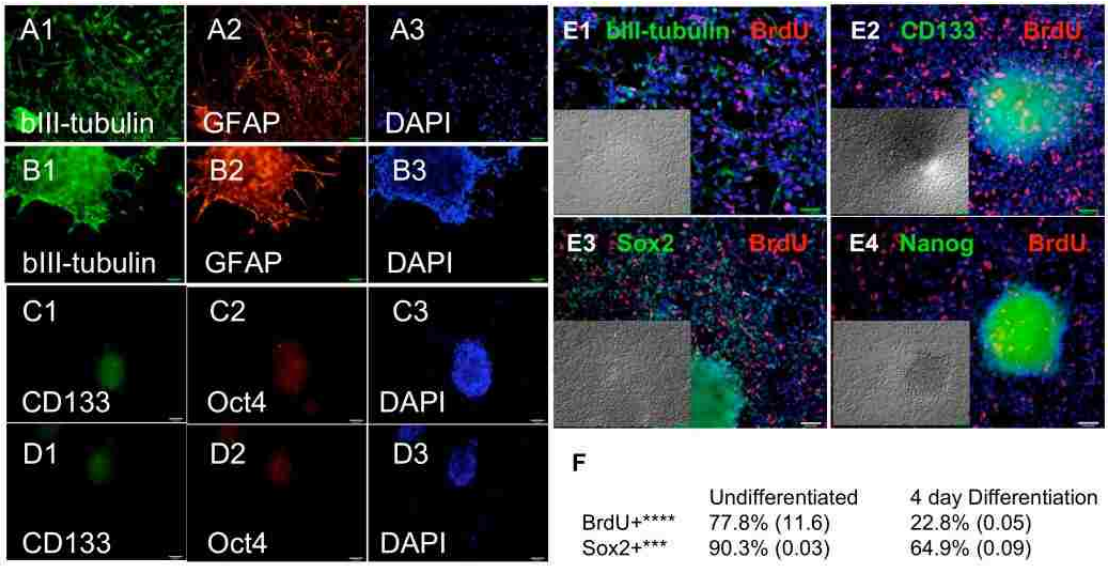

Figure 18: Differentiation of cancer spheroids. Human neural stem cells undergo differentiation when transferred to a serum- and growth factor-free basal medium. Following one week of differentiation in non-supplemented basal cell culture media, neural stem cell spheroids adhered to the plate and migrated outward, increasing the expression of βIII-tubulin (A1) and GFAP (A2), cancer spheroids also expressed βIII-tubulin (B1) and GFAP (B2), but were more resistant to differentiation. Cancer spheroids still expressed stem cell markers CD133 (C1) and Oct4 (C2) after one week of basal media differentiation. Moreover, the expression of both stem cell markers persisted even when cultured in basal media supplemented with retinoic acid (D1-3). The use of serum-supplemented media was used to induce differentiation of tumor spheroids (E1-4). Following four days of serum-induced differentiation, differentiating cells migrated away from the spheroid and had more intense staining for βIII-tubulin (E1), but lower staining for CD133 (E2), Sox2 (E3), and Nanog (E4). Serum-induced differentiation also significantly decreased proliferation and Sox2 expression. Scale bar = 63μm. Statistical significance indicated by asterisks: *p<0.05, **=p<0.01, ***p<0.001, ****p<0.0001.

Culturing gliomas stem cells in serum-supplemented media did facilitate differentiation. Following four days of serum-induced differentiation, cells migrated away from the spheroid and had more intense staining for βIII-tubulin (Figure 18, E1). CD133 expression was still maintained within the intact spheroid, but was not readily detected in the differentiating cells outside the adhered spheroid (Figure 18, E2). Stem cell transcription factors Sox2 (Figure 18, E3) and Nanog (Figure 18, E4) were detected in the spheroid, but only Sox2 expression was observed in the differentiating cells.

Serum-induced differentiation has a significant impact on both the rate of proliferation and expression of stem cell markers (Figure 18, F). Proliferation, as indicated by BrdU-positive staining, showed a significantly decrease in the serum-induced differentiation cultures (22.8%, SD=0.05) compared to the non-differentiated control spheroids (77.8%, SD=11.6, $p<0.0001$). Unlike Nanog, Sox2 was still commonly expressed in the differentiating cells, albeit at a lower frequency compared to undifferentiated cells (90.3%, SD=0.03 compared to 64.9%, SD=0.09, $p<0.0001$).

Rates of proliferation for the adherent and cancer stem cells in vitro were measured by the incorporation of BrdU over a 48-hour period. Immunohistochemical staining revealed a high rate of proliferation for cancer stem cells relative to adherent cells. Specifically, cancer stem cells showed a three to six times higher rate of proliferation relative to adherent cancer cells *in vitro*. Following treatment, 78 percent of cancer stem cells were positive for BrdU, as compared to 24.7 and 13.3 percent for two independent adherent cell lines ($p<0.001$, data not shown).

Effects of Histone Deacetylase Inhibitors on Cancer Stem Cell Lines

When differentiation is induced, proliferation rates and expression of stem cell markers decrease. We therefore hypothesized that a drug that was effective at inducing differentiation would be a promising glioma adjuvant therapy. Although previous studies have demonstrated some anticancer effects of histone deacetylase inhibitors, no one has investigated their effect on glioma stem cells, which are highly resistant to all current chemotherapeutic agents marketed for glioma therapies. We tested the histone deacetylase inhibitors valproic acid and trichostatin A on gene expression and proliferation of cancer stem cells.

Cancer stem cells proliferate rapidly in culture, yielding a high frequency of BrdU-stained cells (Figure 8, A2) as well as robust staining for CD133 (Figure 19, A4). Supplementing the stem cell media for 48 hours with valproic acid (1mM) or trichostatin A (1μM) decreased the number of BrdU-positive cells (Figure 19, B-C2) and showed lower CD133 staining (Figure 8, B-C3). Cells also appear to have more cellular processes after exposure to either VPA (Figure 19, B) or TSA (Figure 19, C), indicating induction of differentiation within a relatively short period of time.

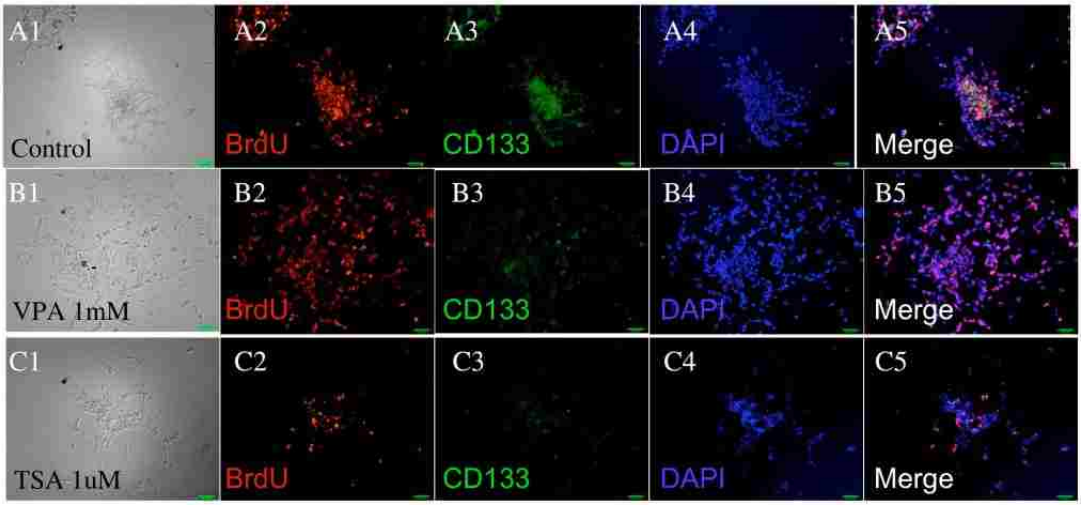

Figure 19: Histone deacetylase inhibitors alter glioma stem cell morphology. Cancer stem cells proliferate rapidly in culture, yielding a high frequency of BrdU-stained cells (A2) as well as robust staining for CD133 (A4). Supplementing the stem cell media with valproic acid (VPA, 1mM) or trichostatin A (TSA, 1μM) decreased the number of BrdU-positive cells (BC2) and showed lower CD133 staining (B-C3). Cells also appear to have more cellular processes after exposure to either VPA (B) or TSA (C), indicating induction of differentiation. Scale bar =63μm.

Treatment with 1mM valproic acid significantly reduced the rate of glioma stem cell proliferation, decreasing the frequency of BrdU-positive cells from 78% to 60% (Figure 20) ($p<0.01$). Exposure to trichostatin A had an even more profound reduction in proliferation, reducing the frequency of cells that underwent proliferation to 34% ($p<0.001$).

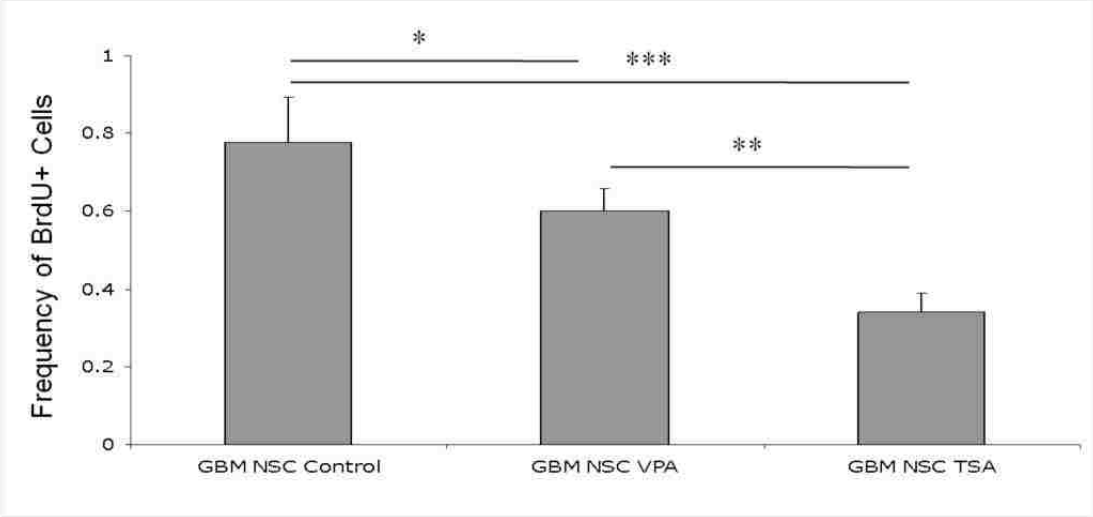

Figure 20: Valproic acid and trichostatin A reduce glioma stem cell proliferation. Treatment with 1mM valproic acid significantly reduced the rate of glioma stem cell proliferation, decreasing the frequency of BrdU-positive cells from 78% to 60% ($p<0.01$). Exposure to trichostatin A had an even more profound reduction in proliferation, reducing the frequency of cells that underwent proliferation to 34% ($p<0.001$).

Treatment with histone deacetylase inhibitors valproic acid and trichostatin A significantly lowered the expression of stem cell genes while increasing the expression of lineage differentiation markers. Expression of CD133 and nanog dramatically reduced when cultured with either VPA (88.0 and 99.8% reduction in CD133 and nanog, $p<0.05$ and $p<0.0001$, respectively) or TSA (86.7% and 99.2%, $p<0.05$ and $p<0.0001$). Valproic acid

inhibited oct4 expression (53.7% reduction, p<0.01), while TSA had a 71% reduction in sox2 levels (p<0.01). The embryonic stem cell marker zfp342 was abated by both drugs (76.2 and 70.1% reduction, p<0.01 and p<0.01). Telomerase reverse transcriptase expression was diminished by both VPA (54.6% reduction, p<0.01) and TSA (80.8% reduction, p<0.05), whereas levels of terf1 were not significantly altered. Interestingly, there were no changes in the levels of the apoptosis inhibitor Bcl-xL or its repressor Bcl-xs. Culturing with the drugs did up-regulate differentiation markers βIII-tubulin (VPA: 2.1x increase, p<0.01) and GFAP (VPA: 3.1x increase, p<0.01, TSA: 4.6x increase, p<0.01) (Figure 21).

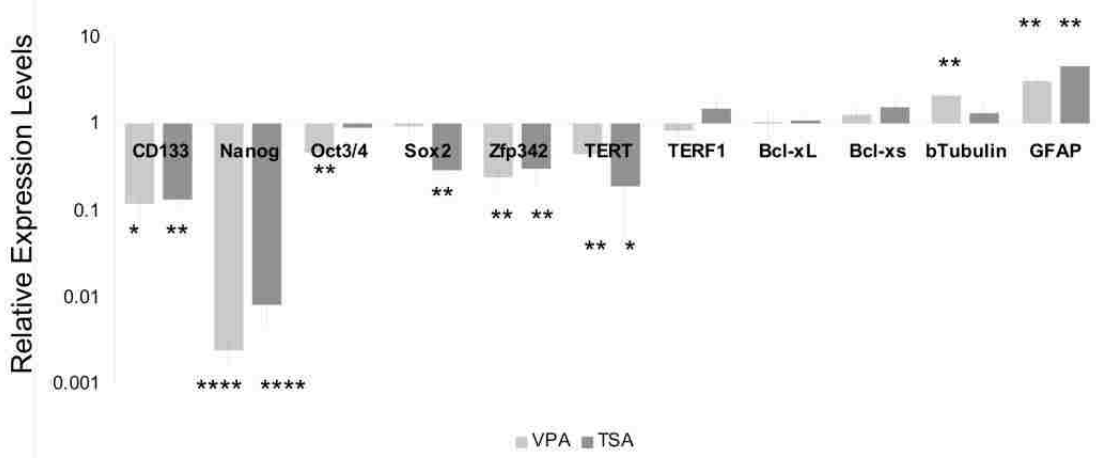

Figure 21: Valproic acid and trichostatin A negatively regulate the expression of stem cell genes. Treatment with histone deacetylase inhibitors valproic acid and trichostatin A significantly lowered the expression of stem cell genes while increasing the expression of lineage differentiation markers. Expression of CD133 and nanog dramatically reduced when cultured with either VPA or TSA. Valproic acid inhibited oct4 expression, while TSA reduced levels of sox2. The embryonic stem cell marker zfp342 was abated by both drugs. TERT was also diminished by both HDACi, whereas levels of terf1 were not significantly altered. Interestingly, there were no changes in the levels of the apoptosis inhibitor Bcl-xL or its repressor Bcl-xs. Culturing with the drugs did up-regulate differentiation markers βIII-tubulin and GFAP.

Discussion

Here we report the ability to generate cancer spheroids from the surgical aspirate of glioblastoma surgeries. The derivation of multiple cell populations from the surgical aspirate offers unique advantages compared to relying on merely the tumor mass. The cells in the aspirate are more disaggregated and avoid the need for extended mechanical dissociation and/or enzymatic digestion. Additionally, viable recovery of multiple cell types may allow for the recovery of healthy neural stem cells that migrate to the tumor. Following rigorous quality control measures, these healthy cells may be transplanted back to the patient to help facilitate recovery, or, given their ability to migrate to tumors, used to deliver anti-tumor compounds.

Potential questions arise regarding differences between cells derived from the tumor mass and those from the surgical aspirate-the later presumably being partially comprised of healthy brain matter. Our studies indicate, at least with respect to the cancer-derived spheroids, that both populations resist differentiation and show rapid rates of proliferation. Following expansion, we believe that there is a selective advantage with the tumor cells relative to the healthy brain cells that are either non-proliferative or display slow cell cycle kinetics. When comparing the two populations, their gene expression profile is surprisingly similar when examining a host of stem cell genes. These stem cells genes have been reportedly expressed in malignant tumors at varying levels, but the similar profile suggests that the spheroids derived from the mass and flush are similar in nature.

Culturing conditions have a large impact on the generation of spheroids in culture. Specifically, culturing cells for 24 hours in serum media produced dramatically more spheroids than culturing directly in neural stem cell media or continuing in culture beyond 24 hours. This skewed distribution suggests that components within the serum may irreversibly change the fate of the stem cells.

The effects of serum on the glioma cell cultures likely skew the cultures in two distinct ways. First, serum induces differentiation of both non-cancerous neural stem cells and glioma-derived stem cells. Therefore, serum culture would quickly eliminate stem cell sub-populations through differentiation. Second, serum-supplemented culture is a radically different environment compared to the in vivo tumor environment. This change in environment causes dramatic changes in gene expression within three passages.[214] In fact, genomic profiling reveals that after only two weeks in culture, seven out of eight glioma samples saw the genomic pattern in adherent serum-based culture diverge from the parent tumor, whereas spheroid suspension cultures preserved the genomic profile of the original tumor.[215]

Gene expression analysis revealed tumor spheroids had significantly higher levels of embryonic stem cell genes including Nanog, Oct4, and Sox2. Although Sox2 is required for neural stem cell maintenance, the expression of Nanog and Oct4 was unexpected since previous reports suggest they are not expressed in neural stem cells. Our own analysis shows that both are not appreciably expressed even in immortalized neural progenitor cell lines.

The higher expression levels of TERT in the cancer stem cell cultures demonstrates the importance of telomerase activity in cancer stem cells and supports the use of it as a clinical marker. However, the elevated expression of TERF1 challenges reports that show TERF1 to be inversely correlated to malignancy. These results, although unexpected, may be explained by three potential hypotheses. First, cancer stem cells are a subpopulation within the tumors, and the lower expression of TERF1 may be the result of a larger percentage of non-cancerous cells comprising the glioma mass. Second, the elevated levels of TERF1 within the cancer stem cells still may be lower than the overall expression in lower grade tumors. Finally, the cancer stem cells may be unresponsive to TERF1, thereby not being affected by higher relative expression. The fact that TERF1 has almost no detection in non-tumor tissues, [216] combined with our data showing no difference in expression following HDACi treatment, suggests a combination of the second and third theories.

Our study demonstrates a clear inhibitory affect of HDACi on glioma stem cells. These data challenges other reports demonstrating an increase in CD133 in gliomas cell lines following treatment with valproic acid and 5-aza-2’deoxycytidine.[217] The authors use commonly available glioma cell lines and convincingly demonstrate that treatment with 5-aza-C and VPA results in promoter hypo-methylation and expression of CD133. However, upon closer inspection of their data, their treatment had the opposite effect in their U87MG cell lines. The U87MG line is unique from the other lines given the higher basal expression of CD133. Moreover, the U87MG line is highly tumorigenic,

readily forming tumors upon transplantation, whereas most glioma cell lines, including the T98G line, are not.[218] The differences observed with the U87MG line are particularly significant since it is the most well-characterized gliomas line containing a sub-population of cancer stem cells.[185, 219-223]

Alternatively, the effects of HDACi may be dependent on p53 status, but that study demonstrated that phenylbutyrate sensitizes glioma cell lines with mutated p53 (U251 and SKMG-3) and did not affect wild-type cells (U87 and D54).[224]

Immunohistochemical staining showed positive staining for CD133 in adherent and cancer spheroids. The expression of CD133 in both populations of cells raises questions regarding its specificity for cancer stem cells. Tumor spheroids and adherent cancer cells show CD133 positive and negative cell populations, although the spheroids are largely positive. Earlier findings suggest that populations of cancer stem cells are CD133 negative, as we have observed. However, the expression of CD133 on the adherent cells, which are far less tumorigenic, suggests that CD133 alone is not a sufficient cancer stem cell marker and/or there is a morphologically distinct population of cancer stem cells. The notable difference between CD133 expression among adherent cell populations may be reflective of differences in the tumor molecular profile, affects of treatment, or a reflection of the surgery.

Conclusions

These markers, given their enrichment in cancer stem cells, may serve as powerful diagnostic and prognostic markers for malignant tumors. The systematic evaluation of these cancer stem cells is important in targeting them for treatment by compounds that selectively induce cell death or make them sensitive to chemotherapy. We demonstrate histone deacetylase inhibitors are effective at inhibiting proliferation and reducing the expression of malignant markers in GBM-derived stem cells, making them a promising therapeutic option.

Author Contributions

A.A. designed and carried out the experiments, generated and analyzed the data, and wrote the manuscript; S.B. provided the fresh tumor samples; K.S. supervised the research and provided critical revisions to the manuscript.

REFERENCES

1. Ferri, C.P., et al., *Global prevalence of dementia: a Delphi consensus study.* Lancet, 2005. **366**(9503): p. 2112-7.

2. Wimo, A., B. Winblad, and L. Jonsson, *An estimate of the total worldwide societal costs of dementia in 2005.* Alzheimers Dement, 2007. **3**(2): p. 81-91.

3. Siwak-Tapp, C.T., et al., *Neurogenesis decreases with age in the canine hippocampus and correlates with cognitive function.* Neurobiol Learn Mem, 2007. **88**(2): p. 249-59.

4. Wati, H., et al., *A decreased survival of proliferated cells in the hippocampus is associated with a decline in spatial memory in aged rats.* Neurosci Lett, 2006. **399**(1-2): p. 171-4.

5. Guidi, S., et al., *Neurogenesis impairment and increased cell death reduce total neuron number in the hippocampal region of fetuses with Down syndrome.* Brain Pathol, 2008. **18**(2): p. 180-97.

6. Kadota, M., Y. Shirayoshi, and M. Oshimura, *Elevated apoptosis in pre-mature neurons differentiated from mouse ES cells containing a single human chromosome 21.* Biochem Biophys Res Commun, 2002. **299**(4): p. 599-605.

7. Zhang, C., et al., *Long-lasting impairment in hippocampal neurogenesis associated with amyloid deposition in a knock-in mouse model of familial Alzheimer's disease.* Exp Neurol, 2007. **204**(1): p. 77-87.

8. Rockenstein, E., et al., *Effects of Cerebrolysin on neurogenesis in an APP transgenic model of Alzheimer's disease.* Acta Neuropathol, 2007. **113**(3): p. 265-75.

9. Nithianantharajah, J. and A.J. Hannan, *Enriched environments, experience-dependent plasticity and disorders of the nervous system.* Nat Rev Neurosci, 2006. **7**(9): p. 697-709.

10. Segovia, G., et al., *Environmental enrichment promotes neurogenesis and changes the extracellular concentrations of glutamate and GABA in the hippocampus of aged rats.* Brain Res Bull, 2006. **70**(1): p. 8-14.

11. Wolf, S.A., et al., *Cognitive and physical activity differently modulate disease progression in the amyloid precursor protein (APP)-23 model of Alzheimer's disease.* Biol Psychiatry, 2006. **60**(12): p. 1314-23.

12. Qu, T., et al., *Human neural stem cells improve cognitive function of aged brain.* Neuroreport, 2001. **12**(6): p. 1127-32.

13. Qu, T.Y., et al., *Bromodeoxyuridine increases multipotency of human bone marrow-derived stem cells.* Restor Neurol Neurosci, 2004. **22**(6): p. 459-68.

14. Srivastava, N., et al., *Long-term functional restoration by neural progenitor cell transplantation in rat model of cognitive dysfunction: co-transplantation with olfactory ensheathing cells for neurotrophic factor support.* Int J Dev Neurosci, 2009. **27**(1): p. 103-10.

15. Wang, Q., et al., *Neural stem cells transplantation in cortex in a mouse model of Alzheimer's disease.* J Med Invest, 2006. **53**(1-2): p. 61-9.

16. Fernandez, C.I., et al., *Motor and cognitive recovery induced by bone marrow stem cells grafted to striatum and hippocampus of impaired aged rats: functional and therapeutic considerations.* Ann N Y Acad Sci, 2004. **1019**: p. 48-52.

17. Bizon, J.L. and M. Gallagher, *Production of new cells in the rat dentate gyrus over the lifespan: relation to cognitive decline.* Eur J Neurosci, 2003. **18**(1): p. 215-9.

18. Bizon, J.L., H.J. Lee, and M. Gallagher, *Neurogenesis in a rat model of age-related cognitive decline.* Aging Cell, 2004. **3**(4): p. 227-34.

19. Juengst, E. and M. Fossel, *The ethics of embryonic stem cells--now and forever, cells without end.* Jama, 2000. **284**(24): p. 3180-4.

20. McLaren, A., *Ethical and social considerations of stem cell research.* Nature, 2001. **414**(6859): p. 129-31.

21. McLaren, A., *Important differences between sources of embryonic stem cells.* Nature, 2000. **408**(6812): p. 513.

22. Barker, R.A. and H. Widner, *Immune problems in central nervous system cell therapy.* NeuroRx, 2004. **1**(4): p. 472-81.

23. Bradley, J.A., E.M. Bolton, and R.A. Pedersen, *Stem cell medicine encounters the immune system.* Nat Rev Immunol, 2002. **2**(11): p. 859-71.

24. Buhnemann, C., et al., *Neuronal differentiation of transplanted embryonic stem cell-derived precursors in stroke lesions of adult rats.* Brain, 2006. **129**(Pt 12): p. 3238-48.

25. Arnhold, S., et al., *Neurally selected embryonic stem cells induce tumor formation after long-term survival following engraftment into the subretinal space.* Invest Ophthalmol Vis Sci, 2004. **45**(12): p. 4251-5.

26. Bieberich, E., et al., *Selective apoptosis of pluripotent mouse and human stem cells by novel ceramide analogues prevents teratoma formation and enriches for neural precursors in ES cell-derived neural transplants.* J Cell Biol, 2004. **167**(4): p. 723-34.

27. Gordeeva, O., et al., *Differentiation of embryonic stem cells after transplantation into peritoneal cavity of irradiated mice and expression of specific germ cell genes in pluripotent cells.* Transplant Proc, 2005. **37**(1): p. 295-8.

28. Rubio, D., et al., *Spontaneous human adult stem cell transformation.* Cancer Res, 2005. **65**(8): p. 3035-9.

29. Jiang, Y., et al., *Neuroectodermal differentiation from mouse multipotent adult progenitor cells.* Proc Natl Acad Sci U S A, 2003. **100 Suppl 1**: p. 11854-60.

30. Jiang, Y., et al., *Pluripotency of mesenchymal stem cells derived from adult marrow.* Nature, 2002. **418**(6893): p. 41-9.

31. Jiang, Y., et al., *Multipotent progenitor cells can be isolated from postnatal murine bone marrow, muscle, and brain.* Exp Hematol, 2002. **30**(8): p. 896-904.

32. Alvarez-Dolado, M., et al., *Fusion of bone-marrow-derived cells with Purkinje neurons, cardiomyocytes and hepatocytes.* Nature, 2003. **425**(6961): p. 968-73.

33. Rodic, N., M.S. Rutenberg, and N. Terada, *Cell fusion and reprogramming: resolving our transdifferences.* Trends Mol Med, 2004. **10**(3): p. 93-6.

34. Terada, N., et al., *Bone marrow cells adopt the phenotype of other cells by spontaneous cell fusion.* Nature, 2002. **416**(6880): p. 542-5.

35. Do, J.T. and H.R. Scholer, *Cell-cell fusion as a means to establish pluripotency.* Ernst Schering Res Found Workshop, 2006(60): p. 35-45.

36. Silva, J., et al., *Nanog promotes transfer of pluripotency after cell fusion.* Nature, 2006. **441**(7096): p. 997-1001.

37. Tada, M. and T. Tada, *Nuclear reprogramming of somatic nucleus hybridized with embryonic stem cells by electrofusion.* Methods Mol Biol, 2006. **329**: p. 411-20.

38. Tada, M., et al., *Nuclear reprogramming of somatic cells by in vitro hybridization with ES cells.* Curr Biol, 2001. **11**(19): p. 1553-8.

39. Do, J.T. and H.R. Scholer, *Comparison of neurosphere cells with cumulus cells after fusion with embryonic stem cells: reprogramming potential.* Reprod Fertil Dev, 2005. **17**(1-2): p. 143-9.

40. Chambers, I., et al., *Functional expression cloning of Nanog, a pluripotency sustaining factor in embryonic stem cells.* Cell, 2003. **113**(5): p. 643-55.

41. Mitsui, K., et al., *The homeoprotein Nanog is required for maintenance of pluripotency in mouse epiblast and ES cells.* Cell, 2003. **113**(5): p. 631-42.

42. Fan, Y., M.F. Melhem, and J.R. Chaillet, *Forced expression of the homeobox-containing gene Pem blocks differentiation of embryonic stem cells.* Dev Biol, 1999. **210**(2): p. 481-96.

43. Eiges, R., et al., *Establishment of human embryonic stem cell-transfected clones carrying a marker for undifferentiated cells.* Curr Biol, 2001. **11**(7): p. 514-8.

44. Niwa, H., J. Miyazaki, and A.G. Smith, *Quantitative expression of Oct-3/4 defines differentiation, dedifferentiation or self-renewal of ES cells.* Nat Genet, 2000. **24**(4): p. 372-6.

45. al Yacoub, N., et al., *Optimized production and concentration of lentiviral vectors containing large inserts.* J Gene Med, 2007. **9**(7): p. 579-84.

46. Mitta, B., M. Rimann, and M. Fussenegger, *Detailed design and comparative analysis of protocols for optimized production of high-performance HIV-1-derived lentiviral particles.* Metab Eng, 2005. **7**(5-6): p. 426-36.

47. Le, Y., et al., *Nuclear targeting determinants of the phage P1 cre DNA recombinase.* Nucleic Acids Res, 1999. **27**(24): p. 4703-9.

48. Le, Y., J.L. Miller, and B. Sauer, *GFPcre fusion vectors with enhanced expression.* Anal Biochem, 1999. **270**(2): p. 334-6.

49. Le, Y. and B. Sauer, *Conditional gene knockout using Cre recombinase.* Mol Biotechnol, 2001. **17**(3): p. 269-75.

50. Livak, K.J. and T.D. Schmittgen, *Analysis of relative gene expression data using real-time quantitative PCR and the 2(-Delta Delta C(T)) Method.* Methods, 2001. **25**(4): p. 402-8.

51. Yuan, J.S., et al., *Statistical analysis of real-time PCR data.* BMC Bioinformatics, 2006. **7**: p. 85.

52. Booth, H.A. and P.W. Holland, *Eleven daughters of NANOG.* Genomics, 2004. **84**(2): p. 229-38.

53. Fairbanks, D.J. and P.J. Maughan, *Evolution of the NANOG pseudogene family in the human and chimpanzee genomes.* BMC Evol Biol, 2006. **6**: p. 12.

54. Hart, A.H., et al., *Identification, cloning and expression analysis of the pluripotency promoting Nanog genes in mouse and human.* Dev Dyn, 2004. **230**(1): p. 187-98.

55. Pain, D., et al., *Multiple retropseudogenes from pluripotent cell-specific gene expression indicates a potential signature for novel gene identification.* J Biol Chem, 2005. **280**(8): p. 6265-8.

56. Zhang, J., et al., *NANOGP8 is a retrogene expressed in cancers.* Febs J, 2006. **273**(8): p. 1723-30.

57. Chew, J.L., et al., *Reciprocal transcriptional regulation of Pou5f1 and Sox2 via the Oct4/Sox2 complex in embryonic stem cells.* Mol Cell Biol, 2005. **25**(14): p. 6031-46.

58. Loh, Y.H., et al., *The Oct4 and Nanog transcription network regulates pluripotency in mouse embryonic stem cells.* Nat Genet, 2006. **38**(4): p. 431-40.

59. Rodda, D.J., et al., *Transcriptional regulation of nanog by OCT4 and SOX2.* J Biol Chem, 2005. **280**(26): p. 24731-7.

60. Kuroda, T., et al., *Octamer and Sox elements are required for transcriptional cis regulation of Nanog gene expression.* Mol Cell Biol, 2005. **25**(6): p. 2475-85.

61. Deb-Rinker, P., et al., *Sequential DNA methylation of the Nanog and Oct-4 upstream regions in human NT2 cells during neuronal differentiation.* J Biol Chem, 2005. **280**(8): p. 6257-60.

62. Perry, P., et al., *A dynamic switch in the replication timing of key regulator genes in embryonic stem cells upon neural induction.* Cell Cycle, 2004. **3**(12): p. 1645-50.

63. Pan, G.J. and D.Q. Pei, *Identification of two distinct transactivation domains in the pluripotency sustaining factor nanog.* Cell Res, 2003. **13**(6): p. 499-502.

64. Suzuki, A., et al., *Nanog binds to Smad1 and blocks bone morphogenetic protein-induced differentiation of embryonic stem cells.* Proc Natl Acad Sci U S A, 2006. **103**(27): p. 10294-9.

65. Pan, G. and D. Pei, *The stem cell pluripotency factor NANOG activates transcription with two unusually potent subdomains at its C terminus.* J Biol Chem, 2005. **280**(2): p. 1401-7.

66. Reyes, M. and C.M. Verfaillie, *Characterization of multipotent adult progenitor cells, a subpopulation of mesenchymal stem cells.* Ann N Y Acad Sci, 2001. **938**: p. 231-3; discussion 233-5.

67. Ulloa-Montoya, F., et al., *Comparative transcriptome analysis of embryonic and adult stem cells with extended and limited differentiation capacity.* Genome Biol, 2007. **8**(8): p. R163.

68. Pan, G., et al., *A negative feedback loop of transcription factors that controls stem cell pluripotency and self-renewal.* Faseb J, 2006. **20**(10): p. 1730-2.

69. Bernardo, M.E., et al., *Human bone marrow derived mesenchymal stem cells do not undergo transformation after long-term in vitro culture and do not exhibit telomere maintenance mechanisms.* Cancer Res, 2007. **67**(19): p. 9142-9.

70. Zimmermann, S., et al., *Lack of telomerase activity in human mesenchymal stem cells.* Leukemia, 2003. **17**(6): p. 1146-9.

71. Eisenberg, L.M. and C.A. Eisenberg, *Stem cell plasticity, cell fusion, and transdifferentiation.* Birth Defects Res C Embryo Today, 2003. **69**(3): p. 209-18.

72. Yamanaka, S., *Induction of pluripotent stem cells from mouse fibroblasts by four transcription factors.* Cell Prolif, 2008. **41 Suppl 1**: p. 51-6.

73. Meissner, A., M. Wernig, and R. Jaenisch, *Direct reprogramming of genetically unmodified fibroblasts into pluripotent stem cells.* Nat Biotechnol, 2007. **25**(10): p. 1177-81.

74. Okita, K., T. Ichisaka, and S. Yamanaka, *Generation of germline-competent induced pluripotent stem cells.* Nature, 2007. **448**(7151): p. 313-7.

75. Takahashi, K., et al., *Induction of pluripotent stem cells from fibroblast cultures.* Nat Protoc, 2007. **2**(12): p. 3081-9.

76. Takahashi, K., et al., *Induction of pluripotent stem cells from adult human fibroblasts by defined factors.* Cell, 2007. **131**(5): p. 861-72.

77. Park, I.H., et al., *Reprogramming of human somatic cells to pluripotency with defined factors.* Nature, 2008. **451**(7175): p. 141-6.

78. Lowry, W.E., et al., *Generation of human induced pluripotent stem cells from dermal fibroblasts.* Proc Natl Acad Sci U S A, 2008. **105**(8): p. 2883-8.

79. Yu, J., et al., *Induced pluripotent stem cell lines derived from human somatic cells.* Science, 2007. **318**(5858): p. 1917-20.

80. Takahashi, K. and S. Yamanaka, *Induction of pluripotent stem cells from mouse embryonic and adult fibroblast cultures by defined factors.* Cell, 2006. **126**(4): p. 663-76.

81. Go, M.J., C. Takenaka, and H. Ohgushi, *Forced expression of Sox2 or Nanog in human bone marrow derived mesenchymal stem cells maintains their expansion and differentiation capabilities.* Exp Cell Res, 2008. **314**(5): p. 1147-54.

82. Sekiya, I., et al., *Expansion of human adult stem cells from bone marrow stroma: conditions that maximize the yields of early progenitors and evaluate their quality.* Stem Cells, 2002. **20**(6): p. 530-41.

83. Sotiropoulou, P.A., et al., *Characterization of the optimal culture conditions for clinical scale production of human mesenchymal stem cells.* Stem Cells, 2006. **24**(2): p. 462-71.

84. Battula, V.L., et al., *Human placenta and bone marrow derived MSC cultured in serum-free, b-FGF-containing medium express cell surface frizzled-9 and SSEA-4 and give rise to multilineage differentiation.* Differentiation, 2007. **75**(4): p. 279-91.

85. Yokoyama, M., et al., *Influence of fetal calf serum on differentiation of mesenchymal stem cells to chondrocytes during expansion.* J Biosci Bioeng, 2008. **106**(1): p. 46-50.

86. Baksh, D., R. Yao, and R.S. Tuan, *Comparison of proliferative and multilineage differentiation potential of human mesenchymal stem cells derived from umbilical cord and bone marrow.* Stem Cells, 2007. **25**(6): p. 1384-92.

87. Haleem-Smith, H., et al., *Optimization of high-efficiency transfection of adult human mesenchymal stem cells in vitro.* Mol Biotechnol, 2005. **30**(1): p. 9-20.

88. Hamm, A., et al., *Efficient transfection method for primary cells.* Tissue Eng, 2002. **8**(2): p. 235-45.

89. McMahon, J.M., et al., *Gene transfer into rat mesenchymal stem cells: a comparative study of viral and nonviral vectors.* Stem Cells Dev, 2006. **15**(1): p. 87-96.

90. Bonab, M.M., et al., *Aging of mesenchymal stem cell in vitro.* BMC Cell Biol, 2006. **7**: p. 14.

91. Moussavi-Harami, F., et al., *Oxygen effects on senescence in chondrocytes and mesenchymal stem cells: consequences for tissue engineering.* Iowa Orthop J, 2004. **24**: p. 15-20.

92. Zhang, X.Y., V.F. La Russa, and J. Reiser, *Transduction of bone-marrow-derived mesenchymal stem cells by using lentivirus vectors pseudotyped with modified RD114 envelope glycoproteins.* J Virol, 2004. **78**(3): p. 1219-29.

93. Greco, S.J., K. Liu, and P. Rameshwar, *Functional similarities among genes regulated by OCT4 in human mesenchymal and embryonic stem cells.* Stem Cells, 2007. **25**(12): p. 3143-54.

94. Wislet-Gendebien, S., et al., *Plasticity of cultured mesenchymal stem cells: switch from nestin-positive to excitable neuron-like phenotype.* Stem Cells, 2005. **23**(3): p. 392-402.

95. Izadpanah, R., et al., *Characterization of multipotent mesenchymal stem cells from the bone marrow of rhesus macaques.* Stem Cells Dev, 2005. **14**(4): p. 440-51.

96. Tsai, M.S., et al., *Clonal amniotic fluid-derived stem cells express characteristics of both mesenchymal and neural stem cells.* Biol Reprod, 2006. **74**(3): p. 545-51.

97. Gonzalez, R., et al., *Pluripotent marker expression and differentiation of human second trimester Mesenchymal Stem Cells.* Biochem Biophys Res Commun, 2007. **362**(2): p. 491-7.

98. Liu, L., et al., *Telomerase deficiency impairs differentiation of mesenchymal stem cells.* Exp Cell Res, 2004. **294**(1): p. 1-8.

99. Parsch, D., et al., *Telomere length and telomerase activity during expansion and differentiation of human mesenchymal stem cells and chondrocytes.* J Mol Med, 2004. **82**(1): p. 49-55.

100. Okamoto, T., et al., *Clonal heterogeneity in differentiation potential of immortalized human mesenchymal stem cells.* Biochem Biophys Res Commun, 2002. **295**(2): p. 354-61.

101. Mori, T., et al., *Combination of hTERT and bmi-1, E6, or E7 induces prolongation of the life span of bone marrow stromal cells from an elderly donor without affecting their neurogenic potential.* Mol Cell Biol, 2005. **25**(12): p. 5183-95.

102. Takeda, Y., et al., *Can the life span of human marrow stromal cells be prolonged by bmi-1, E6, E7, and/or telomerase without affecting cardiomyogenic differentiation?* J Gene Med, 2004. **6**(8): p. 833-45.

103. Abdallah, B.M., et al., *Maintenance of differentiation potential of human bone marrow mesenchymal stem cells immortalized by human telomerase reverse transcriptase gene despite [corrected] extensive proliferation.* Biochem Biophys Res Commun, 2005. **326**(3): p. 527-38.

104. Jun, E.S., et al., *Expression of telomerase extends longevity and enhances differentiation in human adipose tissue-derived stromal cells.* Cell Physiol Biochem, 2004. **14**(4-6): p. 261-8.

105. Kang, S.K., et al., *Expression of telomerase extends the lifespan and enhances osteogenic differentiation of adipose tissue-derived stromal cells.* Stem Cells, 2004. **22**(7): p. 1356-72.

106. Simonsen, J.L., et al., *Telomerase expression extends the proliferative life-span and maintains the osteogenic potential of human bone marrow stromal cells.* Nat Biotechnol, 2002. **20**(6): p. 592-6.

107. Kim, J.B., et al., *Pluripotent stem cells induced from adult neural stem cells by reprogramming with two factors.* Nature, 2008. **454**(7204): p. 646-50.

108. Kim, J.B., et al., *Direct reprogramming of human neural stem cells by OCT4.* Nature, 2009. **461**(7264): p. 649-3.

109. Kim, J.B., et al., *Oct4-induced pluripotency in adult neural stem cells.* Cell, 2009. **136**(3): p. 411-9.

110. Kim, J.B., et al., *Generation of induced pluripotent stem cells from neural stem cells.* Nat Protoc, 2009. **4**(10): p. 1464-70.

111. Sugaya, K., *Neuroreplacement therapy and stem cell biology under disease conditions.* Cell Mol Life Sci, 2003. **60**(9): p. 1891-902.

112. Sugaya, K., et al., *Stem cell strategies for Alzheimer's disease therapy.* Panminerva Med, 2006. **48**(2): p. 87-96.

113. Kwak, Y.D., et al., *Amyloid precursor protein regulates differentiation of human neural stem cells.* Stem Cells Dev, 2006. **15**(3): p. 381-9.

114. Kwak, Y.D., E. Choumkina, and K. Sugaya, *Amyloid precursor protein is involved in staurosporine induced glial differentiation of neural progenitor cells.* Biochem Biophys Res Commun, 2006. **344**(1): p. 431-7.

115. Marutle, A., et al., *Modulation of human neural stem cell differentiation in Alzheimer (APP23) transgenic mice by phenserine.* Proc Natl Acad Sci U S A, 2007. **104**(30): p. 12506-11.

116. Lassman, A.B., et al., *Overexpression of c-MYC promotes an undifferentiated phenotype in cultured astrocytes and allows elevated Ras and Akt signaling to induce gliomas from GFAP-expressing cells in mice.* Neuron Glia Biol, 2004. **1**(2): p. 157-63.

117. Stupp, R., et al., *Changing paradigms--an update on the multidisciplinary management of malignant glioma.* Oncologist, 2006. **11**(2): p. 165-80.

118. Fine, H.A., et al., *Meta-analysis of radiation therapy with and without adjuvant chemotherapy for malignant gliomas in adults.* Cancer, 1993. **71**(8): p. 2585-97.

119. Walker, M.D., T.A. Strike, and G.E. Sheline, *An analysis of dose-effect relationship in the radiotherapy of malignant gliomas.* Int J Radiat Oncol Biol Phys, 1979. **5**(10): p. 1725-31.

120. Simpson, J.R., et al., *Influence of location and extent of surgical resection on survival of patients with glioblastoma multiforme: results of three consecutive Radiation Therapy Oncology Group (RTOG) clinical trials.* Int J Radiat Oncol Biol Phys, 1993. **26**(2): p. 239-44.

121. Huncharek, M. and J. Muscat, *Treatment of recurrent high grade astrocytoma; results of a systematic review of 1,415 patients.* Anticancer Res, 1998. **18**(2B): p. 1303-11.

122. Lacroix, M., et al., *A multivariate analysis of 416 patients with glioblastoma multiforme: prognosis, extent of resection, and survival.* J Neurosurg, 2001. **95**(2): p. 190-8.

123. Stupp, R., et al., *Promising survival for patients with newly diagnosed glioblastoma multiforme treated with concomitant radiation plus temozolomide followed by adjuvant temozolomide.* J Clin Oncol, 2002. **20**(5): p. 1375-82.

124. Stupp, R., et al., *Radiotherapy plus concomitant and adjuvant temozolomide for glioblastoma.* N Engl J Med, 2005. **352**(10): p. 987-96.

125. Tait, M.J., et al., *Survival of patients with glioblastoma multiforme has not improved between 1993 and 2004: analysis of 625 cases.* Br J Neurosurg, 2007. **21**(5): p. 496-500.

126. Groothuis, D.R., *The blood-brain and blood-tumor barriers: a review of strategies for increasing drug delivery.* Neuro Oncol, 2000. **2**(1): p. 45-59.

127. Neuwelt, E.A., *Mechanisms of disease: the blood-brain barrier.* Neurosurgery, 2004. **54**(1): p. 131-40; discussion 141-2.

128. Bigner, D.D., et al., *Heterogeneity of Genotypic and phenotypic characteristics of fifteen permanent cell lines derived from human gliomas.* J Neuropathol Exp Neurol, 1981. **40**(3): p. 201-29.

129. Kurpad, S.N., et al., *Tumor antigens in astrocytic gliomas.* Glia, 1995. **15**(3): p. 244-56.

130. Vick, W.W., et al., *The use of a panel of monoclonal antibodies in the evaluation of cytologic specimens from the central nervous system.* Acta Cytol, 1987. **31**(6): p. 815-24.

131. Galli, R., et al., *Isolation and characterization of tumorigenic, stem-like neural precursors from human glioblastoma.* Cancer Res, 2004. **64**(19): p. 7011-21.

132. Jordan, C.T., M.L. Guzman, and M. Noble, *Cancer stem cells.* N Engl J Med, 2006. **355**(12): p. 1253-61.

133. Qiang, L., et al., *Isolation and characterization of cancer stem like cells in human glioblastoma cell lines.* Cancer Lett, 2009.

134. Singh, S.K., et al., *Identification of a cancer stem cell in human brain tumors.* Cancer Res, 2003. **63**(18): p. 5821-8.

135. Singh, S.K., et al., *Identification of human brain tumour initiating cells.* Nature, 2004. **432**(7015): p. 396-401.

136. Yuan, X., et al., *Isolation of cancer stem cells from adult glioblastoma multiforme.* Oncogene, 2004. **23**(58): p. 9392-400.

137. Noble, M. and J. Dietrich, *Intersections between neurobiology and oncology: tumor origin, treatment and repair of treatment-associated damage.* Trends Neurosci, 2002. **25**(2): p. 103-7.

138. Zhang, Q.B., et al., *Differentiation profile of brain tumor stem cells: a comparative study with neural stem cells.* Cell Res, 2006. **16**(12): p. 909-15.

139. Kania, G., et al., *Somatic stem cell marker prominin-1/CD133 is expressed in embryonic stem cell-derived progenitors.* Stem Cells, 2005. **23**(6): p. 791-804.

140. Uchida, N., et al., *Direct isolation of human central nervous system stem cells.* Proc Natl Acad Sci U S A, 2000. **97**(26): p. 14720-5.

141. Lee, A., et al., *Isolation of neural stem cells from the postnatal cerebellum.* Nat Neurosci, 2005. **8**(6): p. 723-9.

142. Barraud, P., et al., *In vitro characterization of a human neural progenitor cell coexpressing SSEA4 and CD133.* J Neurosci Res, 2007. **85**(2): p. 250-9.

143. Pfenninger, C.V., et al., *CD133 is not present on neurogenic astrocytes in the adult subventricular zone, but on embryonic neural stem cells, ependymal cells, and glioblastoma cells.* Cancer Res, 2007. **67**(12): p. 5727-36.

144. Aboody, K.S., et al., *Neural stem cells display extensive tropism for pathology in adult brain: evidence from intracranial gliomas.* Proc Natl Acad Sci U S A, 2000. **97**(23): p. 12846-51.

145. Tang, Y., et al., *In vivo tracking of neural progenitor cell migration to glioblastomas.* Hum Gene Ther, 2003. **14**(13): p. 1247-54.

146. Zhang, Z., et al., *In vivo magnetic resonance imaging tracks adult neural progenitor cell targeting of brain tumor.* Neuroimage, 2004. **23**(1): p. 281-7.

147. Armstrong, R.C., et al., *Pre-oligodendrocytes from adult human CNS.* J Neurosci, 1992. **12**(4): p. 1538-47.

148. Eriksson, P.S., et al., *Neurogenesis in the adult human hippocampus.* Nat Med, 1998. **4**(11): p. 1313-7.

149. Nunes, M.C., et al., *Identification and isolation of multipotential neural progenitor cells from the subcortical white matter of the adult human brain.* Nat Med, 2003. **9**(4): p. 439-47.

150. Pringle, N.P., et al., *PDGF receptors in the rat CNS: during late neurogenesis, PDGF alpha-receptor expression appears to be restricted to glial cells of the oligodendrocyte lineage.* Development, 1992. **115**(2): p. 535-51.

151. Roy, N.S., et al., *Identification, isolation, and promoter-defined separation of mitotic oligodendrocyte progenitor cells from the adult human subcortical white matter.* J Neurosci, 1999. **19**(22): p. 9986-95.

152. Sanai, N., et al., *Unique astrocyte ribbon in adult human brain contains neural stem cells but lacks chain migration.* Nature, 2004. **427**(6976): p. 740-4.

153. Shoshan, Y., et al., *Expression of oligodendrocyte progenitor cell antigens by gliomas: implications for the histogenesis of brain tumors.* Proc Natl Acad Sci U S A, 1999. **96**(18): p. 10361-6.

154. Kim, S.U., *Antigen expression by glial cells grown in culture.* J Neuroimmunol, 1985. **8**(4-6): p. 255-82.

155. Goings, G.E., V. Sahni, and F.G. Szele, *Migration patterns of subventricular zone cells in adult mice change after cerebral cortex injury.* Brain Res, 2004. **996**(2): p. 213-26.

156. Kim, S.K., et al., *PEX-producing human neural stem cells inhibit tumor growth in a mouse glioma model.* Clin Cancer Res, 2005. **11**(16): p. 5965-70.

157. Kim, S.K., et al., *Human neural stem cells target experimental intracranial medulloblastoma and deliver a therapeutic gene leading to tumor regression.* Clin Cancer Res, 2006. **12**(18): p. 5550-6.

158. Bao, S., et al., *Stem cell-like glioma cells promote tumor angiogenesis through vascular endothelial growth factor.* Cancer Res, 2006. **66**(16): p. 7843-8.

159. Liu, G., et al., *Analysis of gene expression and chemoresistance of CD133+ cancer stem cells in glioblastoma.* Mol Cancer, 2006. **5**: p. 67.

160. Rich, J.N., *Cancer stem cells in radiation resistance.* Cancer Res, 2007. **67**(19): p. 8980-4.

161. Dietrich, J., et al., *Clinical patterns and biological correlates of cognitive dysfunction associated with cancer therapy.* Oncologist, 2008. **13**(12): p. 1285-95.

162. Argyriou, A.A., et al., *Either Called "Chemobrain" or "Chemofog," the Long-Term Chemotherapy-Induced Cognitive Decline in Cancer Survivors Is Real.* J Pain Symptom Manage.

163. Shiras, A., et al., *Spontaneous transformation of human adult nontumorigenic stem cells to cancer stem cells is driven by genomic*

instability in a human model of glioblastoma. Stem Cells, 2007. **25**(6): p. 1478-89.

164. Lin, T., et al., *p53 induces differentiation of mouse embryonic stem cells by suppressing Nanog expression.* Nat Cell Biol, 2005. **7**(2): p. 165-71.

165. Xu, Y., *A new role for p53 in maintaining genetic stability in embryonic stem cells.* Cell Cycle, 2005. **4**(3): p. 363-4.

166. Laws, E.R., et al., *Survival following surgery and prognostic factors for recently diagnosed malignant glioma: data from the Glioma Outcomes Project.* J Neurosurg, 2003. **99**(3): p. 467-73.

167. van den Bent, M.J., M.E. Hegi, and R. Stupp, *Recent developments in the use of chemotherapy in brain tumours.* Eur J Cancer, 2006. **42**(5): p. 582-8.

168. Beier, D., et al., *CD133(+) and CD133(-) glioblastoma-derived cancer stem cells show differential growth characteristics and molecular profiles.* Cancer Res, 2007. **67**(9): p. 4010-5.

169. Salmaggi, A., et al., *Glioblastoma-derived tumorospheres identify a population of tumor stem-like cells with angiogenic potential and enhanced multidrug resistance phenotype.* Glia, 2006. **54**(8): p. 850-60.

170. Singh, S.K., et al., *Cancer stem cells in nervous system tumors.* Oncogene, 2004. **23**(43): p. 7267-73.

171. Gunther, H.S., et al., *Glioblastoma-derived stem cell-enriched cultures form distinct subgroups according to molecular and phenotypic criteria.* Oncogene, 2008. **27**(20): p. 2897-909.

172. Bao, S., et al., *Glioma stem cells promote radioresistance by preferential activation of the DNA damage response.* Nature, 2006. **444**(7120): p. 756-60.

173. Kang, M.K., et al., *Potential identity of multi-potential cancer stem-like subpopulation after radiation of cultured brain glioma.* BMC Neurosci, 2008. **9**: p. 15.

174. Shervington, A. and C. Lu, *Expression of multidrug resistance genes in normal and cancer stem cells.* Cancer Invest, 2008. **26**(5): p. 535-42.

175. Murat, A., et al., *Stem cell-related "self-renewal" signature and high epidermal growth factor receptor expression associated with resistance*

to concomitant chemoradiotherapy in glioblastoma. J Clin Oncol, 2008. **26**(18): p. 3015-24.

176. Svendsen, C.N., et al., *A new method for the rapid and long term growth of human neural precursor cells.* J Neurosci Methods, 1998. **85**(2): p. 141-52.

177. Breier, J.M., et al., *Development of a high-throughput screening assay for chemical effects on proliferation and viability of immortalized human neural progenitor cells.* Toxicol Sci, 2008. **105**(1): p. 119-33.

178. Donato, R., et al., *Differential development of neuronal physiological responsiveness in two human neural stem cell lines.* BMC Neurosci, 2007. **8**: p. 36.

179. Rychlik, W., *OLIGO 7 primer analysis software.* Methods Mol Biol, 2007. **402**: p. 35-60.

180. Rozen, S. and H. Skaletsky, *Primer3 on the WWW for general users and for biologist programmers.* Methods Mol Biol, 2000. **132**: p. 365-86.

181. Untergasser, A., et al., *Primer3Plus, an enhanced web interface to Primer3.* Nucleic Acids Res, 2007. **35**(Web Server issue): p. W71-4.

182. Aerts, J.L., M.I. Gonzales, and S.L. Topalian, *Selection of appropriate control genes to assess expression of tumor antigens using real-time RT-PCR.* Biotechniques, 2004. **36**(1): p. 84-6, 88, 90-1.

183. Gerard, C.J., et al., *Improved quantitation of minimal residual disease in multiple myeloma using real-time polymerase chain reaction and plasmid-DNA complementarity determining region III standards.* Cancer Res, 1998. **58**(17): p. 3957-64.

184. Huggett, J., et al., *Real-time RT-PCR normalisation; strategies and considerations.* Genes Immun, 2005. **6**(4): p. 279-84.

185. Nakai, E., et al., *Enhanced MDR1 Expression and Chemoresistance of Cancer Stem Cells Derived from Glioblastoma.* Cancer Invest, 2009: p. 1.

186. Schmittgen, T.D. and B.A. Zakrajsek, *Effect of experimental treatment on housekeeping gene expression: validation by real-time, quantitative RT-PCR.* J Biochem Biophys Methods, 2000. **46**(1-2): p. 69-81.

187. Vlassenbroeck, I., et al., *Validation of real-time methylation-specific PCR to determine O6-methylguanine-DNA methyltransferase gene promoter methylation in glioma.* J Mol Diagn, 2008. **10**(4): p. 332-7.

188. Appelskog, I.B., et al., *Histone deacetylase inhibitor 4-phenylbutyrate suppresses GAPDH mRNA expression in glioma cells.* Int J Oncol, 2004. **24**(6): p. 1419-25.

189. Giricz, O., J.L. Lauer-Fields, and G.B. Fields, *The normalization of gene expression data in melanoma: investigating the use of glyceraldehyde 3-phosphate dehydrogenase and 18S ribosomal RNA as internal reference genes for quantitative real-time PCR.* Anal Biochem, 2008. **380**(1): p. 137-9.

190. Lyng, M.B., et al., *Identification of genes for normalization of real-time RT-PCR data in breast carcinomas.* BMC Cancer, 2008. **8**: p. 20.

191. Berkman, R.A., et al., *Clonal composition of glioblastoma multiforme.* J Neurosurg, 1992. **77**(3): p. 432-7.

192. Skaper, S.D. and J.E. Seegmiller, *Elevated intracellular glycine associated with hypoxanthine-guanine phosphoribosyltransferase deficiency in glioma cells.* J Neurochem, 1977. **29**(1): p. 83-6.

193. Brannen, C.L. and K. Sugaya, *In vitro differentiation of multipotent human neural progenitors in serum-free medium.* Neuroreport, 2000. **11**(5): p. 1123-8.

194. Das, A., N.L. Banik, and S.K. Ray, *Retinoids induced astrocytic differentiation with down regulation of telomerase activity and enhanced sensitivity to taxol for apoptosis in human glioblastoma T98G and U87MG cells.* J Neurooncol, 2008. **87**(1): p. 9-22.

195. Loo, D.T., M.C. Althoen, and C.W. Cotman, *Differentiation of serum-free mouse embryo cells into astrocytes is accompanied by induction of glutamine synthetase activity.* J Neurosci Res, 1995. **42**(2): p. 184-91.

196. Marchal-Victorion, S., et al., *The human NTERA2 neural cell line generates neurons on growth under neural stem cell conditions and exhibits characteristics of radial glial cells.* Mol Cell Neurosci, 2003. **24**(1): p. 198-213.

197. Cikos, S., A. Bukovska, and J. Koppel, *Relative quantification of mRNA: comparison of methods currently used for real-time PCR data analysis.* BMC Mol Biol, 2007. **8**: p. 113.

198. Vrotsos, E.G., P.E. Kolattukudy, and K. Sugaya, *MCP-1 involvement in glial differentiation of neuroprogenitor cells through APP signaling.* Brain Res Bull, 2009. **79**(2): p. 97-103.

199. Vrotsos, E.G. and K. Sugaya, *MCP-1-induced migration of NT2 neuroprogenitor cells involving APP signaling.* Cell Mol Neurobiol, 2009. **29**(3): p. 373-81.

200. Student, *The probable error of a mean.* Biometrika, 1908. **6**(1): p. 1-25.

201. Zimmerman, D.W., *A note on preliminary tests of equality of variances.* Br J Math Stat Psychol, 2004. **57**(Pt 1): p. 173-81.

202. Welch, B.L., *The Significance of the Difference Between Two Means when the Population Variances are UnequalThe Significance of the Difference Between Two Means when the Population Variances are Unequal.* Biometrika, 1938. **29**(3/4): p. 350-62.

203. Welch, B.L., *The Generalization of `Student's' Problem when Several Different Population Variances are Involved.* Biometrika, 1947. **34**(1/2): p. 28-35.

204. Jeanmougin, M., et al., *Should we abandon the t-test in the analysis of gene expression microarray data: a comparison of variance modeling strategies.* PLoS One. **5**(9): p. e12336.

205. Rieu, I. and S.J. Powers, *Real-time quantitative RT-PCR: design, calculations, and statistics.* Plant Cell, 2009. **21**(4): p. 1031-3.

206. Estes, M.L., et al., *Characterization of adult human astrocytes derived from explant culture.* J Neurosci Res, 1990. **27**(4): p. 697-705.

207. McKeever, P.E., et al., *Products of cells cultured from gliomas. V. Cytology and morphometry of two cell types cultured from glioma.* J Natl Cancer Inst, 1987. **78**(1): p. 75-84.

208. Rutka, J.T., et al., *Establishment and characterization of five cell lines derived from human malignant gliomas.* Acta Neuropathol, 1987. **75**(1): p. 92-103.

209. Wang, J., et al., *Establishment of a new human glioblastoma multiforme cell line (WJ1) and its partial characterization.* Cell Mol Neurobiol, 2007. **27**(7): p. 831-43.

210. Besser, D., *Expression of nodal, lefty-a, and lefty-B in undifferentiated human embryonic stem cells requires activation of Smad2/3.* J Biol Chem, 2004. **279**(43): p. 45076-84.

211. Postovit, L.M., et al., *Human embryonic stem cell microenvironment suppresses the tumorigenic phenotype of aggressive cancer cells.* Proc Natl Acad Sci U S A, 2008. **105**(11): p. 4329-34.

212. Smith, J.R., et al., *Inhibition of Activin/Nodal signaling promotes specification of human embryonic stem cells into neuroectoderm.* Dev Biol, 2008. **313**(1): p. 107-17.

213. Tabibzadeh, S. and A. Hemmati-Brivanlou, *Lefty at the crossroads of "stemness" and differentiative events.* Stem Cells, 2006. **24**(9): p. 1998-2006.

214. Lee, J., et al., *Tumor stem cells derived from glioblastomas cultured in bFGF and EGF more closely mirror the phenotype and genotype of primary tumors than do serum-cultured cell lines.* Cancer Cell, 2006. **9**(5): p. 391-403.

215. De Witt Hamer, P.C., et al., *The genomic profile of human malignant glioma is altered early in primary cell culture and preserved in spheroids.* Oncogene, 2008. **27**(14): p. 2091-6.

216. La Torre, D., et al., *Expression of telomeric repeat binding factor-1 in astroglial brain tumors.* Neurosurgery, 2005. **56**(4): p. 802-10.

217. Tabu, K., et al., *Promoter hypomethylation regulates CD133 expression in human gliomas.* Cell Res, 2008. **18**(10): p. 1037-46.

218. Ishii, N., et al., *Frequent co-alterations of TP53, p16/CDKN2A, p14ARF, PTEN tumor suppressor genes in human glioma cell lines.* Brain Pathol, 1999. **9**(3): p. 469-79.

219. Aguado, T., et al., *Cannabinoids induce glioma stem-like cell differentiation and inhibit gliomagenesis.* J Biol Chem, 2007. **282**(9): p. 6854-62.

220. Annabi, B., et al., *Modulation of invasive properties of CD133+ glioblastoma stem cells: a role for MT1-MMP in bioactive lysophospholipid signaling.* Mol Carcinog, 2009. **48**(10): p. 910-9.

221. Annabi, B., et al., *A MT1-MMP/NF-kappaB signaling axis as a checkpoint controller of COX-2 expression in CD133+ U87 glioblastoma cells.* J Neuroinflammation, 2009. **6**: p. 8.

222. Yao, X.H., et al., *Glioblastoma stem cells produce vascular endothelial growth factor by activation of a G-protein coupled formylpeptide receptor FPR.* J Pathol, 2008. **215**(4): p. 369-76.

223. Yu, S.C., et al., *Isolation and characterization of cancer stem cells from a human glioblastoma cell line U87.* Cancer Lett, 2008. **265**(1): p. 124-34.

224. Lopez, C.A., et al., *Phenylbutyrate sensitizes human glioblastoma cells lacking wild-type p53 function to ionizing radiation.* Int J Radiat Oncol Biol Phys, 2007. **69**(1): p. 214-20.